UCRL-ID-113316

Forensic Analyses of Explosion Debris from the January 2, 1992 Pd/D_2O Electrochemistry Incident at SRI International

Brian Andresen
Richard Whipple
Dick Vandervoort
Patrick Grant

A Public Domain Report to
California Division of Occupational Safety and Health

August 15, 1992

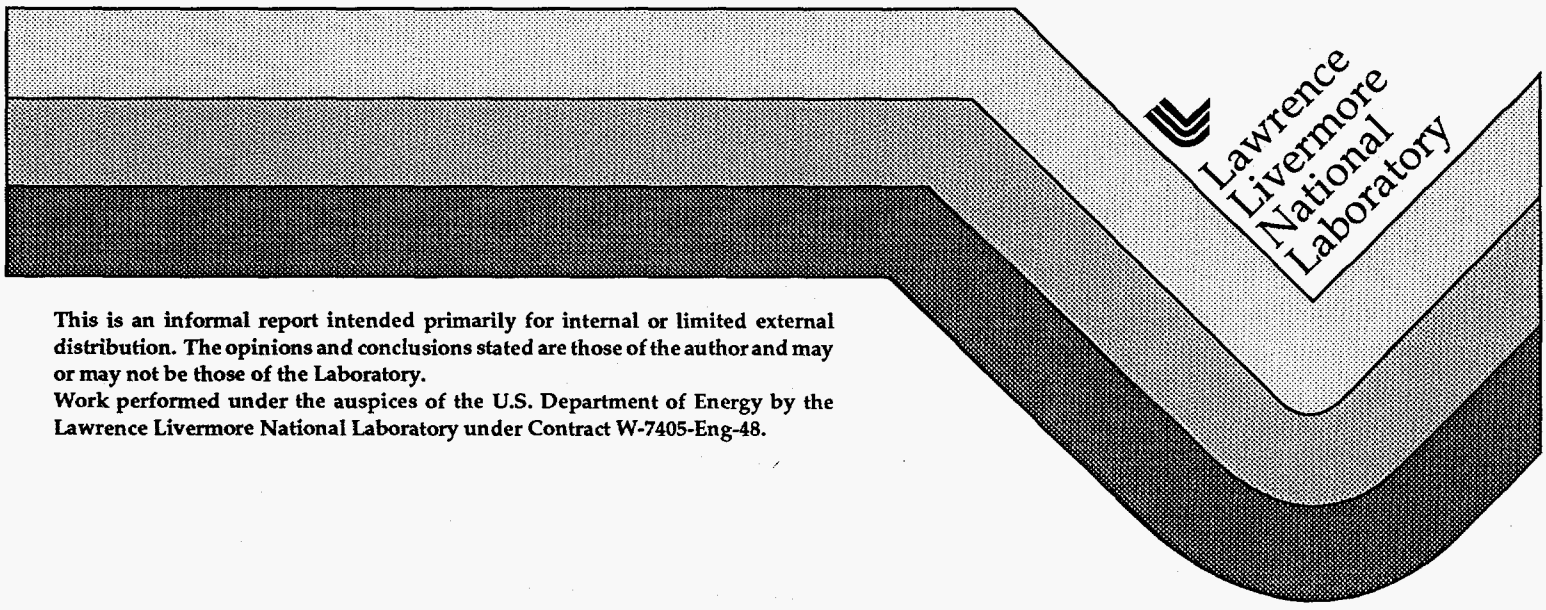

DISCLAIMER

* The principal project coordinators and authors of this report were:

Brian Andresen, Director, LLNL Forensic Science Center

Rich Whipple, Explosives Specialist, LLNL Forensic Science Center

Dick Vandervoort, LLNL Engineering Sciences Division

Patrick Grant, LLNL Nuclear Chemistry Division

However, the analytical work implemented to interrogate the various components of the explosion debris required a multidisciplinary effort that transcended traditional scientific boundaries at the Laboratory. The individual analysts and scientific personnel contributing to this work are listed on the following page. They were thus the members of the LLNL Forensic Science Team for this project.

LLNL Forensic Science Team for the SRI Incident Analyses

LBL
Rick Russo
Elton Cairns

Special Projects
Dave Dye
Jared DuFresne
Ellen Raber
Jerry Wood
Jerry Johnson

Envir. Sci. Div.
Jim Brunk
Kai Wong

Lab. Legal
Gerry Richards
Bill DeGarmo

Public Affairs
Gordon Yano

Tech. Transfer
Gib Marguth
Hallie Gibson

Foren. Sci. Center
Brian Andresen
Rich Whipple
Jackie Stilwell
Jeff Haas
Armando Alcaraz
Rod Eagle
Terry Freitas

Chem. & Mat. Sci.
Chuck Otto
Rich Torres
Nora Butler
Carlos Colmenares
Cheryl Evans
Allison Connor
Trish Baisden

LLNL Institutional
Bob Andrews
Roger Werne
Tony Chargin
Ron Cochran
Lamar Coleman

Nucl. Chem. Div.
Doug Leich
Doug Phinney
Dave Smith
Chuck Bazan
Jeff Chandler
Sid Niemeyer
Dick Nagle
Bob Lanier
Carol Velsko
John Andrews
Zach Koenig
Pat Grant

Combustion Phys.
Craig Tarver
Paul Urtiew
Charlie Westbrook
Bill Pitz

Mech. Engin.
Steve Root
Dick Ryon
Dick Vandervoort
Greg Bianchini
Richard Meagher
Bob Kershaw
Bill Fritts
Lin Hester
Ken Dolan
Gene Ford
Gerry Sobczak
Zig Jandrisevits
Harry Martz
Satish Kulkarni
Edwin Sedillo
Brian Kelly

REPORT SECTIONS

1. Introduction

2. Nuclear Analyses and Results
   - Preliminary Comments
   - Counting Methodology
   - γ-Spectrometry Results

3. Chemical and Physical Sampling Methods

4. Inorganic Chemistry Analyses and Results
   - Sample Pretreatments
   - Tritium Analyses
   - ICP-MS Analyses
   - Ion Chromatography Analyses
   - Conclusions

5. Organic Chemistry Analyses and Results
   - Preliminary Comments
   - Sample Pretreatment
   - GC-MS Analyses
   - Conclusions
   - Supplementary Remarks

6. Particulate Analyses
   - Preliminary Comments
   - Electron and Ion Microprobe Analyses
   - ESCA Analyses

7. Materials Characterization and Structural Analyses
   - Nondestructive XRF Analyses
   - High-Energy X-Ray Radiography
   - Post-Explosion Cell Dimensions
   - Metallurgical Analyses

8. Summary

INTRODUCTION

INTRODUCTION

In early April 1992, Lawrence Livermore National Laboratory (LLNL) began a dialog with California's Division of Occupational Safety and Health (Cal-OSHA) through the intermediary efforts of Dr. Rick Russo of the Lawrence Berkeley National Laboratory. As part of an incident investigation, Cal-OSHA desired the analytical interrogation of debris material confiscated by the Menlo Park Fire Department after the January 2, 1992 explosion in an electrochemistry laboratory at SRI International (SRI). The explosion resulted in the death of scientist Andrew Riley, and gained some notoriety due to its association with experimental work in the controversial field of "cold fusion" research. [Throughout this report, the term "cold fusion" is used as a convenient descriptor for electrolysis experiments designed to study the generation of excess heat by currently unknown mechanisms; whether conventional nuclear fusion might be a contributing factor to this phenomenon is problematical at the present time.]

LLNL agreed in principle to serve as an objective, third-party analytical laboratory for forensic analyses of the SRI debris. The primary motivation for LLNL's assistance to the State of California in this matter is the Laboratory's commitment to service in the public interest. In addition, however, as a major nuclear facility within the U.S. Department of Energy, LLNL has had an inherent curiosity in the novelty of "cold fusion" since its announcement in 1989. Although the existing forensic capabilities of LLNL are quite substantial, past implementations of this expertise have been predominantly in the realms of national security, defense, and intelligence operations. With the remarkable recent changes in the international environment and the end of the Cold War, a focus on more conventional applications of forensic science could provide productive areas of opportunity for future Laboratory activities.

On April 16, 1992, Cal-OSHA transferred custody of the explosion debris to LLNL, and two Livermore staff members transported the material from OSHA Headquarters to LLNL. We comment here that the evidence was handled extensively by several people and organizations before receipt by LLNL, and the detailed history of these examinations is largely unknown to us. This fact may or may not be influential in the results of the forensic analyses, but present thinking is that it is probably only a minor effect in the overall analytic scenario.

The evidence was placed in a locked repository within the LLNL Forensic Science Center, except for the emplacement of a cylinder of D_2 gas in a laboratory fume hood. We remark that some of the interesting debris remained

in SRI's possession after the incident. These included the electrochemical palladium (Pd) electrodes as well as platinum-coated alumina (Al_2O_3) catalytic spheres. SRI is conducting their own independent investigation of the incident.

For the next several weeks, the only analysis performed on the debris was nondestructive gamma-ray spectroscopy of selected metallic components. A variety of legal exercises and identification of appropriate funding sources for the LLNL analyses culminated on May 7, 1992 with the signature of LLNL's Laboratory Counsel to a Cal-OSHA Confidentiality Agreement. In an attempt to elucidate underlying mechanisms or contributing factors to the explosion, forensic analysis of the SRI debris began on May 8, 1992.

Initial, detailed inspection of the debris at LLNL was observed by Dr. Fran Tanzella of SRI, and subsequent discussions between him and LLNL analysts were productive and cordial. The components of the debris were weighed and photographed at this time. Selected photographs from the layout are presented at the end of this section of this report.

The more interesting pieces of debris (the main, stainless-steel cell vessel, the detached cell base, and the ripped Teflon liner) were then sampled for ensuing inorganic, organic, and physical analyses at the LLNL Forensic Science Center. Finally, interrogation of various debris components for structural integrity and materials characterization was performed by LLNL radiography, metallurgical, and engineering personnel. The results of the nuclear, chemical, physical, and engineering analyses performed at LLNL are presented in this report.

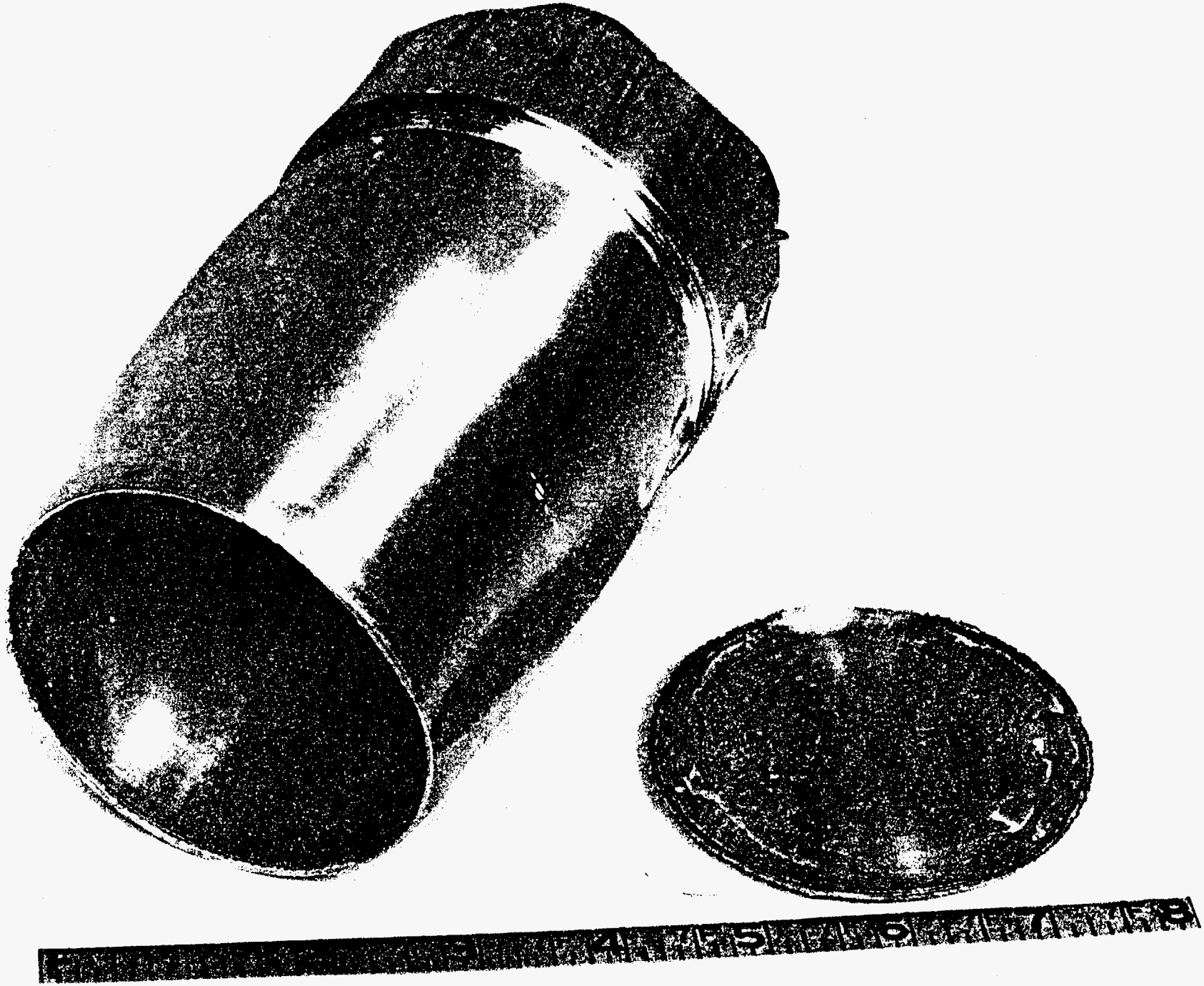

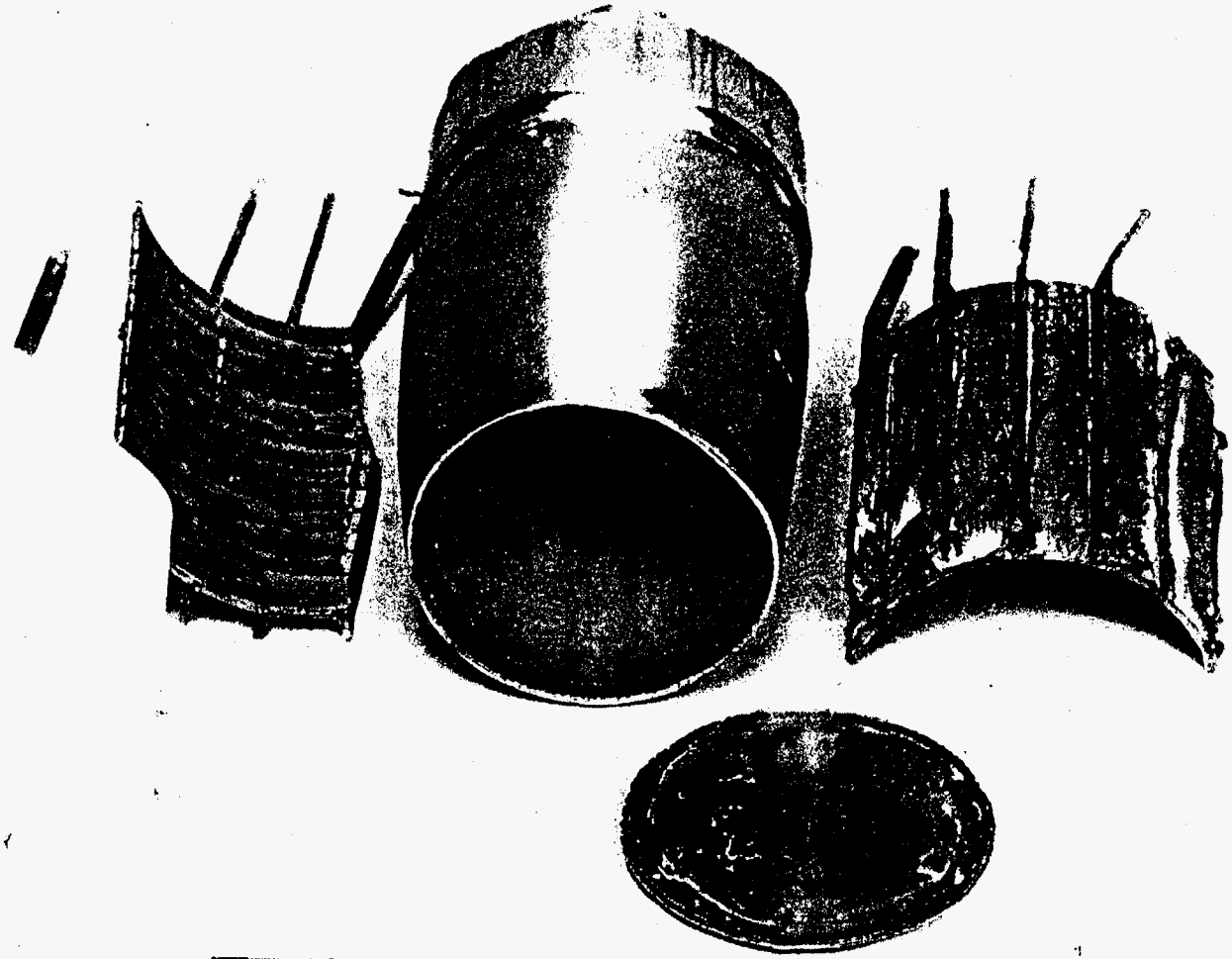

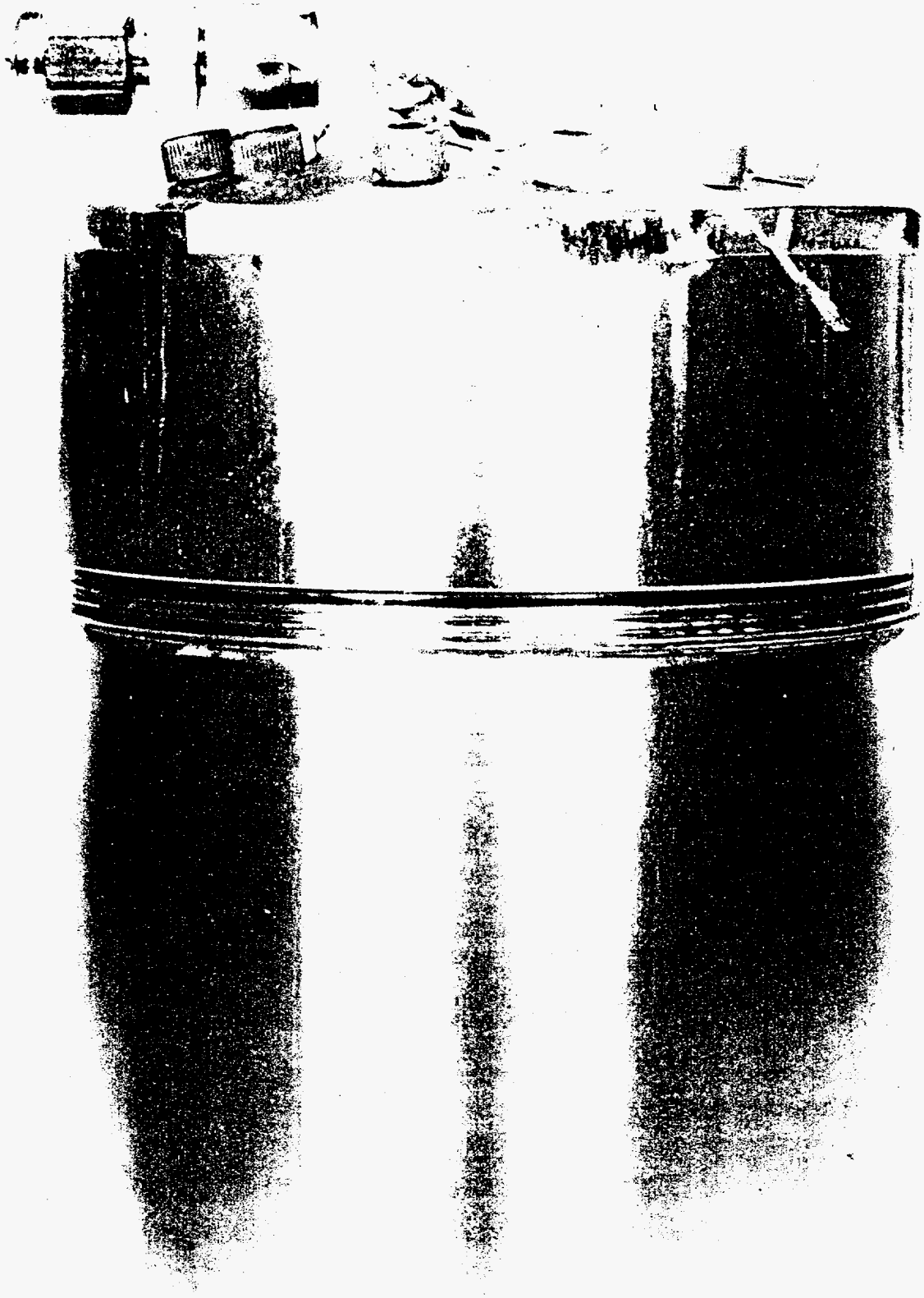

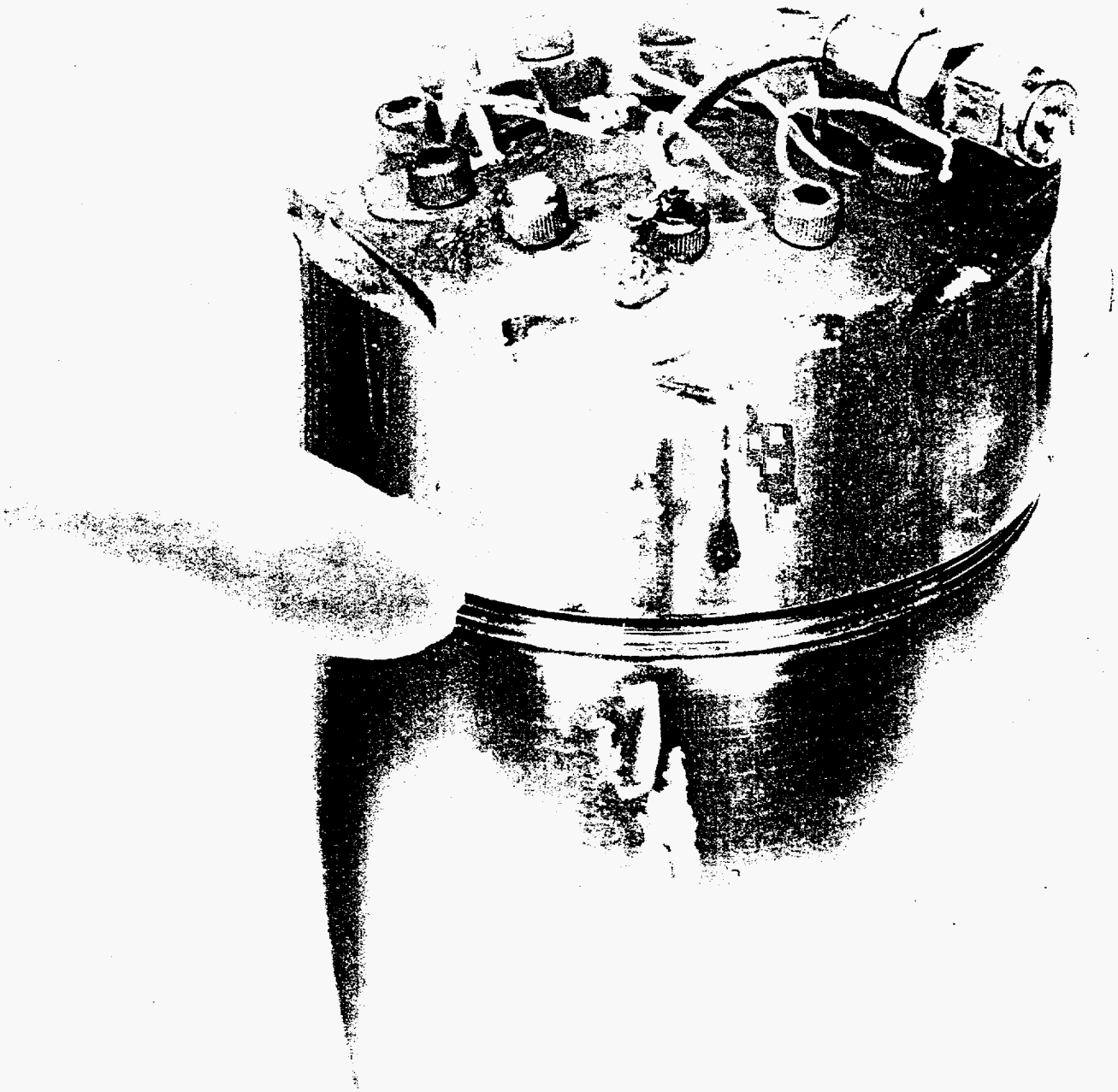

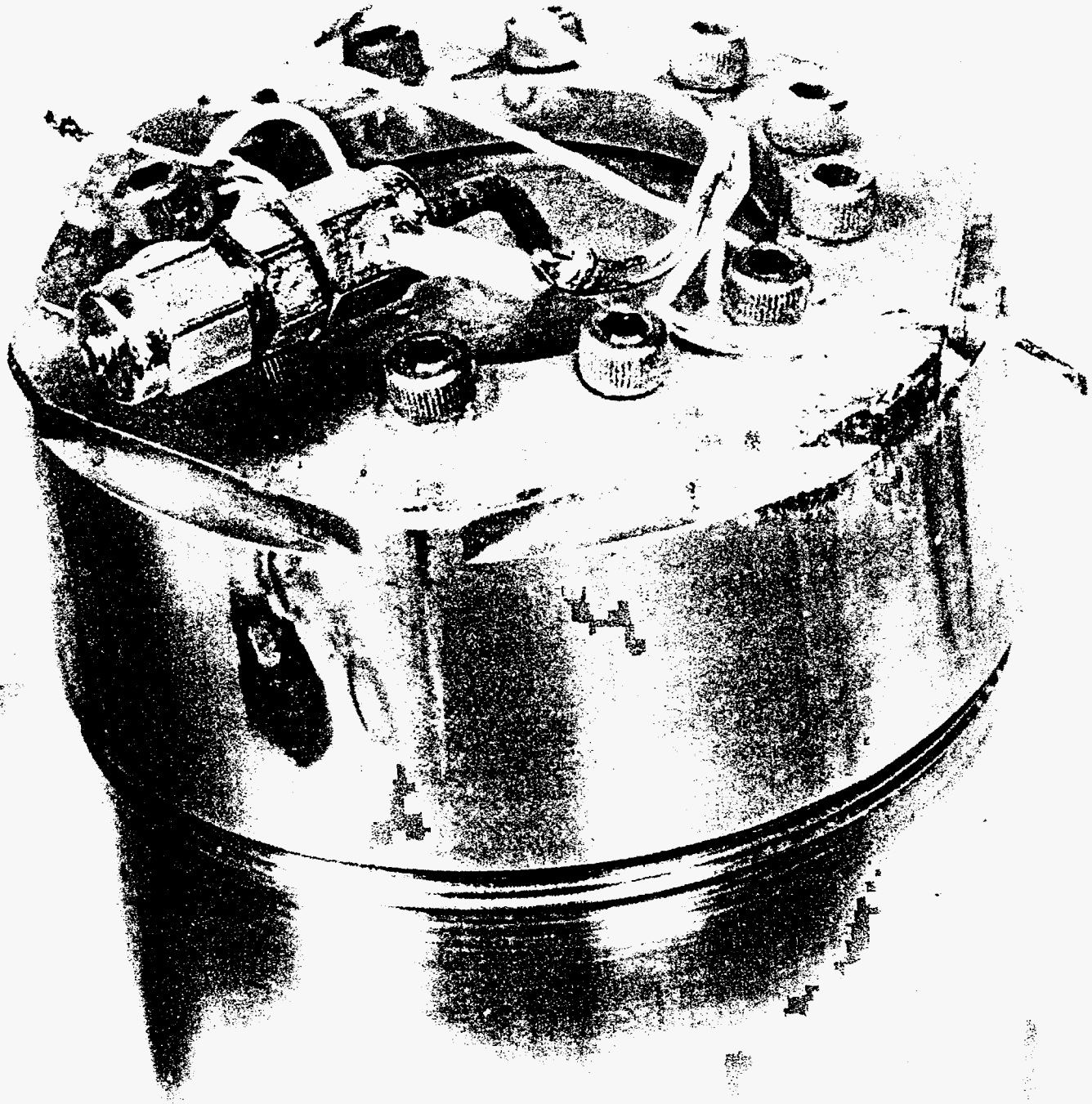

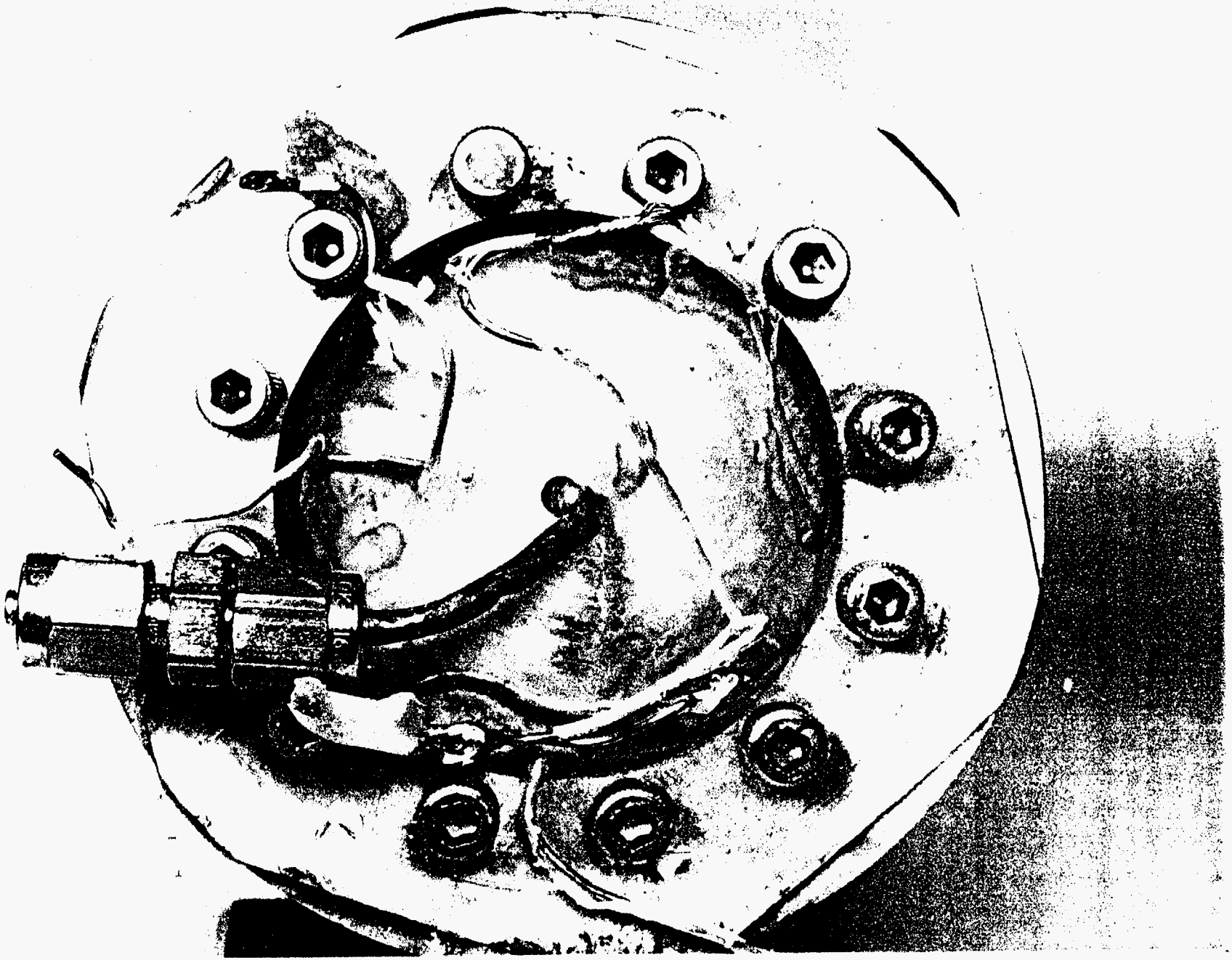
mm 10 20 30 40 50 60 70 80 90 100 110

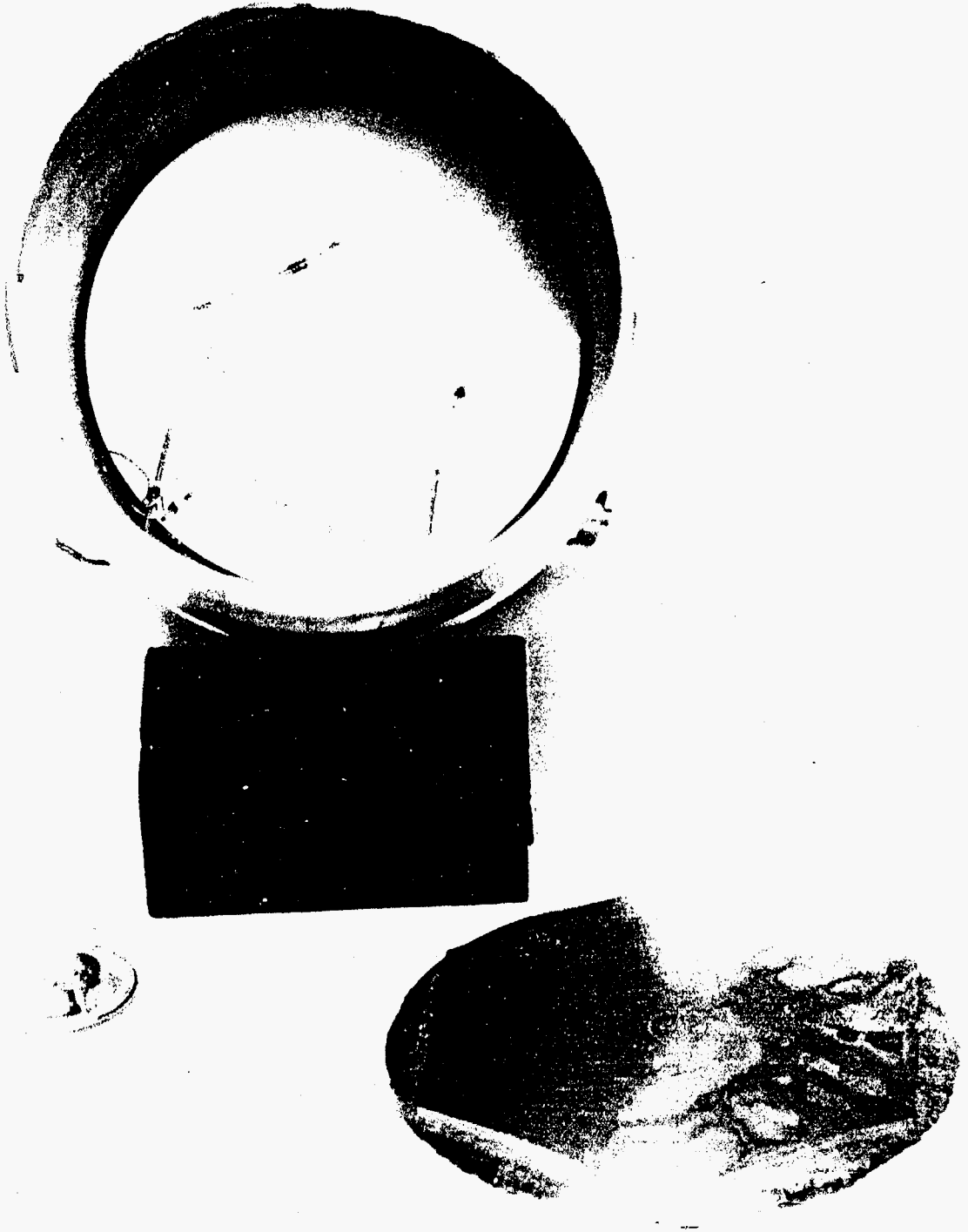

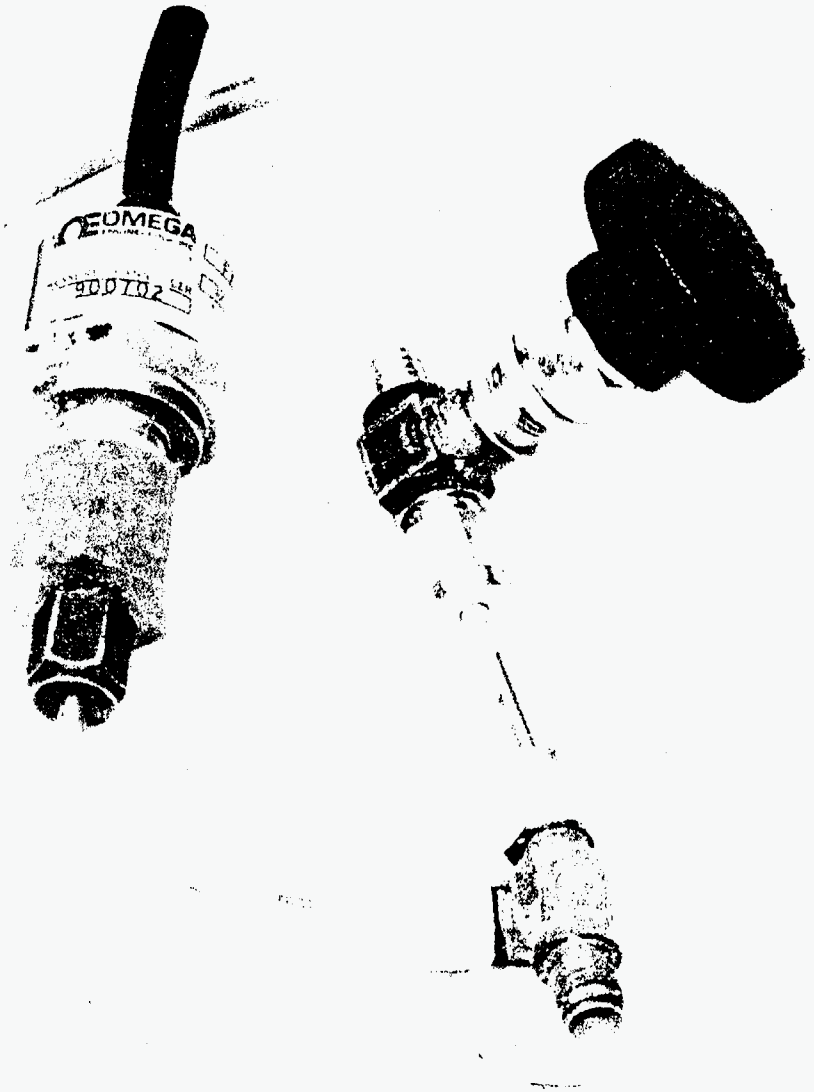

1E . 1 . 7IF 2 . 7IF 3 . 7IF 4 . 7IF 5 . 7IF 6 . 7IF 7 .

NUCLEAR

NUCLEAR ANALYSES AND RESULTS

Preliminary Comments

In the short history of "cold fusion" experimentation, perhaps the most contentious claims from various laboratories involve an association of excess heat generation with the presence or absence of signature species indicative of known nuclear processes. These nuclear signatures have included the production of neutrons, tritium, ^{4}He, and prompt gamma (γ) rays. Of these, the generation of neutrons as fusion by-products appears to be gaining some acceptance among the skeptics of "cold fusion." For example, a recent report claims that on the order of 50 laboratories around the world have detected the presence of neutron emission in their electrochemical experiments.

If a burst of neutrons was associated with the SRI explosion, it is possible that detectable activation products were produced in the surrounding materials. With a sufficiently high neutron fluence, radioactivity induced in the near environment might be detected and discriminated from background radiation by nondestructive γ-ray spectrometry. Such analyses are superbly and conveniently performed at LLNL on a routine basis.

The components of the debris judged most likely to contain residual induced activity were the distended, stainless-steel, electrolysis cell vessel and the brass fins of the heat-exchanger. At Cal-OSHA Headquarters in San Francisco, two separate γ-ray counting packages were defined and triply-bagged with heavy, zip-locked, plastic bags before transport to LLNL. These packages were:

1) the distended cell with the threaded cap and bolts intact and still assembled as one piece; the detached cell base was included in this package, and the total weight was 1.78 kg; hereafter in this section of the report, this counting specimen will be referred to as the "SS cell."

2) two reasonably intact heat-exchanger fins along with fragments of other fins; the heat-transfer structure was assembled in a clamshell fit around the SS cell at the time of the explosion; the weight of this counting package was 562 g but did not include the portion of the heat-exchanger debris that remained with SRI after the incident; this counting specimen will be referred to as the "brass fins."

As an initial caveat for these studies, we comment that neither stainless steel nor brass are very sensitive materials for neutron activation investigations. The reasons for this statement encompass considerations of metal

compositions, the fractional abundance of appropriate stable target nuclides, and the half-lives and gamma energies (i.e., the "detectability") of candidate activation products. Moreover, the incident neutron energy spectrum would be an important parameter in any analysis of radioactivation, and contemplation of this factor for this particular incident would be distinguished by conjecture and uncertainty. A search for the presence of nuclear reaction products induced by either thermal or fast neutrons was consequently the object of these analyses.

Nuclear analyses at LLNL did not commence until approximately 3.5 months after the incident. Any short-lived radionuclides that may have been present at earlier times would not have been detected by LLNL's γ-ray spectroscopic investigations. Unfortunately, it is these short-lifetime activities that would have provided the most sensitive interrogation of the debris for a potential neutron pulse.

Counting Methodology

The outer plastic bag was removed from each counting sample, and each specimen was centered on the detector face of a low-background, γ-ray spectrometer system in LLNL's Environmental Sciences Division (ESD). The SS cell was counted for 3.78 days in a position of maximum efficiency on spectrometer system "EG," while the brass fins were similarly analyzed on system "FE" for 2.78 days. The samples were then transported to the Nuclear Chemistry Division (NCD) for similar analysis on the ultrahigh sensitivity system "II-BW" in an isolated, low-background area of the basement counting wing. The second plastic bag was removed, and the SS cell was counted for 6.67 days on the NCD spectrometer. This same procedure was then followed for the brass fins, which were γ-counted for 6.75 days. At both the ESD and NCD locations, long system background counts were effected immediately after spectral interrogation of the analyte samples.

Spectrometer system settings and data reduction of the γ spectra were basically equivalent at both the ESD and NCD counting facilities. As efficiency-calibrated, constant-geometry configurations were impossible with these debris specimens, qualitative counts of the samples as close to the detectors as possible were the basic goals of the γ analyses. The spectrometers interrogated the γ spectrum from approximately 50-2000 keV with 4096-channel pulse-height analyzers at a system gain of 0.5 keV/channel. Spectral data were recorded on magnetic tape, and computer analysis of photopeak energy and intensity information was accomplished with the GAMANAL program code.

The performance parameters of the various spectrometer systems utilized in this work were somewhat different, however, and traditional figures-of-merit for the ESD and NCD γ detectors used here are presented in the following table.

γ-Spectrometry Results

A nominal zero-time for the SRI incident was approximately 11:45 a.m. on January 2, 1992 [day 2.531(92) PDT in NCD nomenclature]. All of the γ spectra of the SS cell and brass fins measured at LLNL were acquired at times ranging from 109 to 120.4 days after zero-time. Potential neutron activation products with half-lives sufficiently long to survive this decay time are summarized in the next table, and they were the primary analytes of interest in these studies.

A representative γ spectrum, obtained from the week-long count of the SS cell, is shown in the accompanying figure. None of the spectra measured at LLNL gave any indication of residual radioactivity attributable to neutron-induced nuclear reactions in the SS cell or brass fins. All photopeaks identified by GAMANAL in the 50-2000 keV region could be assigned to background radiation, and the identities of these background activities were primarily 511-keV annihilation radiation, ^{40}K, ^{232}Th daughter nuclides, and ^{238}U daughters.

Based on statistical analysis of Compton background data in appropriate regions of a spectrum, GAMANAL can calculate limits-of-detection for selected radionuclides in any given count. These computations require accurate detector efficiency data as a function of photopeak energy, however, and these data depend in turn on well-calibrated counting configurations utilizing primary γ-ray standards. Well-specified counting geometries were impossible with the irregular shapes of the SRI debris. Nevertheless, very gross and simplistic approximations to the counting efficiencies were implemented to make semi-quantitative estimates of limits-of-detection. Results from these exercises should be considered order-of-magnitude numbers at best.

With these comments as prologue, the upper detection limits assigned by GAMANAL to the various activation products listed in the preceding table are conveyed here. For the ESD γ spectra, limits-of-detection for the analyte species in the counting samples were on the order of pCi at the time of the counts. For the NCD data, because of superior detector efficiency and longer acquisition times, the limits-of-detection for the candidate activation products were an order of magnitude better at 0.1 pCi. We emphasize that no candidate γ photopeaks were observed; the appropriate energy regions of the various

Performance Parameters of γ Detectors Utilized at LLNL for the Interrogation of Explosion Debris Samples						
LLNL Division	ID	Detector Type	Values at 1333 keV of ^{60}Co Decay			
			Relative Efficiency (%)	FWHM (keV)	FWTM (keV)	Peak/Compton
Environmental Sciences (ESD)	EG	Ge(Li)	18.8	2.00	3.78	42:1
ESD	FE	Ge	21.8	1.75	3.31	55:1
Nuclear Chemistry (NCD)	II-BW	Ge	40.0	1.94	3.62	58:1

Potential Neutron Activation Products in SRI Debris at Decay Times of 3-4 Months					
Element (nominal composition in weight %)	Stable Target Nuclide (% abundance)	Nuclear Reaction	Product Nuclide	Half-Life	E_γ in keV (I_γ in %)
Type 316 Stainless Steel					
Fe (60-70%)	^{54}Fe (5.8%)	(n,p)	^{54}Mn	312 d	835 (100%)
	^{54}Fe (5.8%)	(n,α)	^{51}Cr	27.7 d	320 (10%)
	^{58}Fe (0.3%)	(n,γ)	^{59}Fe	44.5 d	1099 (56%), 1292 (44%)
Cr (16-18%)	^{50}Cr (4.4%)	(n,γ)	^{51}Cr		
	^{52}Cr (84%)	(n,2n)	^{51}Cr		
Ni (10-14%)	^{58}Ni (68%)	(n,pn)	^{57}Co	272 d	122 (86%), 136 (11%)
	^{58}Ni (68%)	(n,p)	^{58}Co	70.8 d	811 (99%)
	^{60}Ni (26%)	(n,p)	^{60}Co	5.27 y	1173 (100%), 1333 (100%)
	^{61}Ni (1.1%)	(n,pn)	^{60}Co		
	^{62}Ni (3.6%)	(n,α)	^{59}Fe		
Mo (2-3%)	^{92}Mo (15%)	(n,pn)	^{91}Nb	61 d	1205 (4%)
	^{92}Mo (15%)	(n,p)	^{92}Nb	10.2 d	934 (99%)
	^{95}Mo (16%)	(n,p)	^{95}Nb	35.1 d	766 (100%)
	^{96}Mo (17%)	(n,pn)	^{95}Nb		
	^{98}Mo (24%)	(n,α)	^{95}Zr	64.0 d	724 (44%), 757 (55%)
Mn (<2%)	^{55}Mn (100%)	(n,2n)	^{54}Mn		
Brass					
Cu (67%)	^{63}Cu (69%)	(n,α)	^{60}Co		
Zn (33%)	^{64}Zn (49%)	(n,γ)	^{65}Zn	244 d	1116 (51%)
	^{66}Zn (28%)	(n,2n)	^{65}Zn		

SRI SS Electrolysis Cell

Ge Gamma–Ray Spectrum

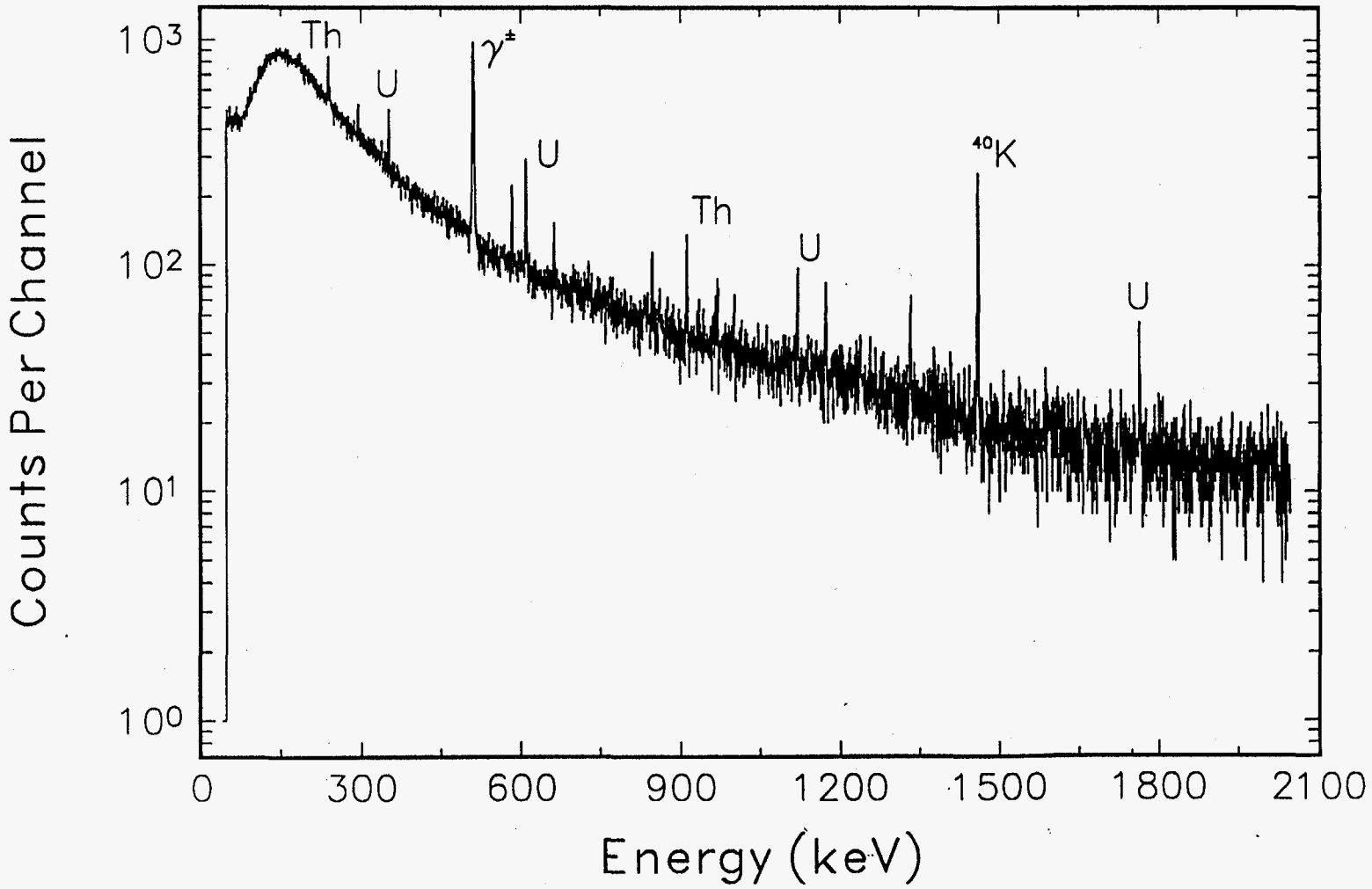

spectra revealed only random data distributions about a slowly varying Compton background.

Thus, within the time and materials limitations discussed above, no evidence for the presence of neutrons associated with the SRI explosion was observed at LLNL.

SAMPLING

CHEMICAL & PHYSICAL SAMPLING METHODS

The pieces of debris sampled for chemical and physical analyses were the stainless-steel (SS) cell vessel (with threaded cap intact), the detached SS cell base, and the ripped Teflon liner. Small, particulate residues were removed from the interior of the cell vessel with scapula and forceps, and they were transferred to a small reagent bottle. These particles from the cell interior could be visually grouped into white, black, and brownish components. As is visible in photographs in the Introduction section, a very small quantity of white residue was caked on the interior surface of the detached cell base. This material had to be pared into a reagent bottle with a scapula, and it appeared more homogeneous and fragile than the particles from the interior of the main cell vessel. A photomicrographic record of these specimens was obtained, and representative photos are shown at the end of this section.

Following removal of the particulate samples, the SS vessel, the detached base, and the ripped Teflon liner were each divided into four quadrants for chemical sampling of the specimens' interiors. One quadrant was wiped for organic residues with absorbent paper saturated with 3:1 $CH_2Cl_2/CH_3CHOHCH_3$ solvent, another quadrant was wiped with paper and 0.05 M HNO_3 for inorganic residues, and a third quadrant was wiped with paper and 0.05 M NaOH, also for trace inorganic species. The fourth quadrant was left undisturbed for possible future interrogation by another laboratory, if desired. For the purposes of the chemical sampling, the interior of the SS cell vessel was separated into two distinct components: 1) the SS wall; and 2) a Teflon end-piece still intact in the cell cap, with holes and protruding wires visible upon viewing from the base of the open cell (see photo in Introduction).

The debris parts sampled for organic and inorganic chemical analyses were thus the interior portions of: 1) the Teflon end-piece in the cell cap; 2) the SS cell vessel walls; 3) the detached SS base; and 4) the ripped Teflon liner. Those numbers were also those assigned for sample identification purposes in the chemical analyses (i.e., SRI-2 indicates a sample from the SS cell vessel walls, etc.). Appropriate blank specimens for all wipe procedures were generated at the time of the sampling and were designated with the number 5.

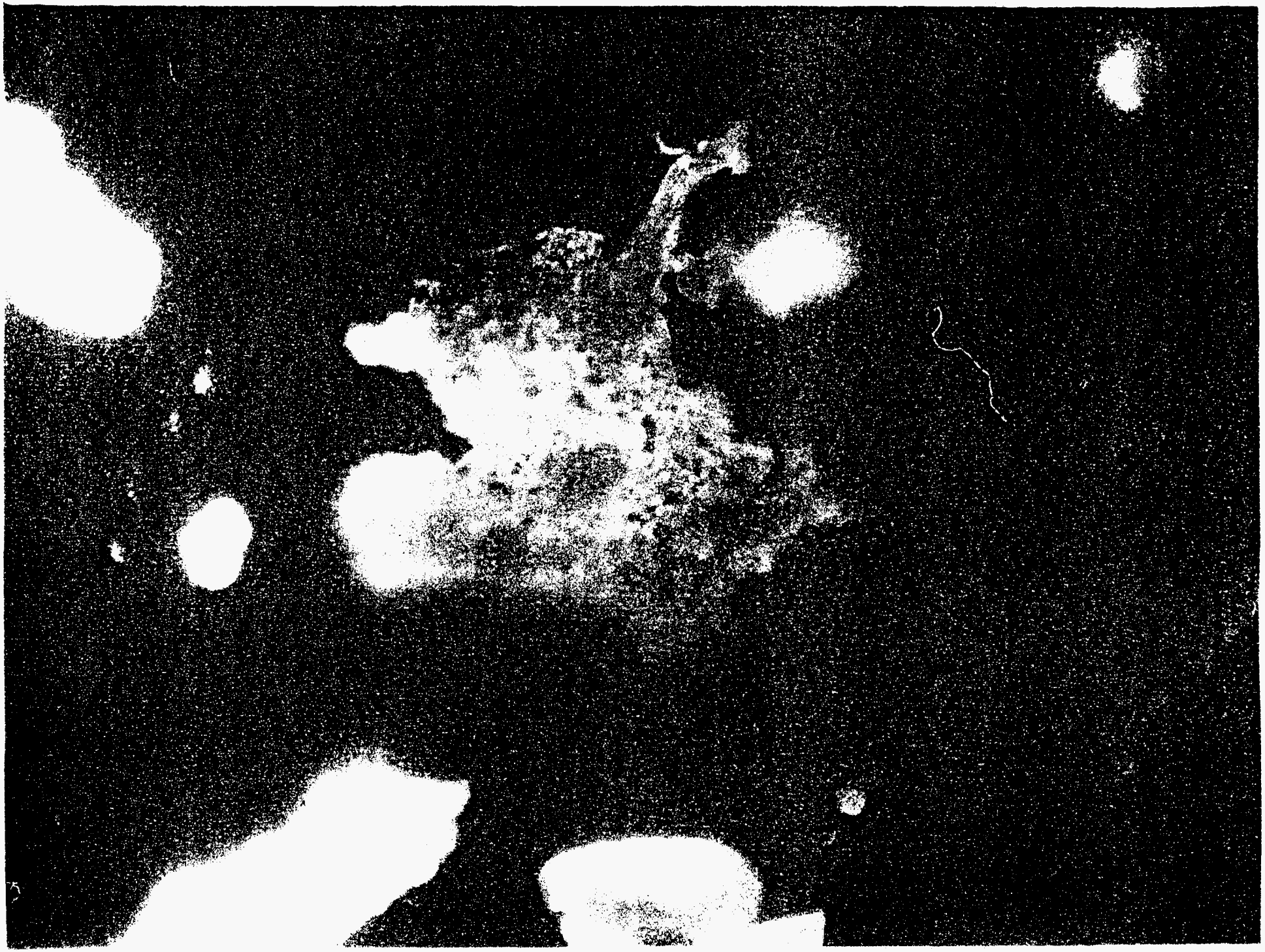

INORGANIC

INORGANIC CHEMISTRY ANALYSES AND RESULTS

The purpose of these analyses was to search for any unusual elemental or inorganic species that might be present in the debris. Although not expected from what is presently known about this incident, LLNL easily and routinely interrogates diverse samples for residual evidence of propellant or conventional explosive signatures. These tests are very sensitive and were conducted here for completeness of the overall analysis.

Sample Pretreatments

The wipes from the four debris components and the blank were chemically manipulated to convert the samples to forms suitable for instrumental inorganic analyses. Each acid specimen (0.05 M HNO_3) was transferred quantitatively to a 125-ml Erlenmeyer flask, and the absorbent paper was wet-ashed with concentrated HNO_3 and $HClO_4$. The residue was then dissolved in 4 M HNO_3 and centrifuged at 2000 rpm. The supernate from the centrifugation was transferred to a 50-ml class "A" volumetric flask and diluted to the mark with 4 M HNO_3. Aliquots from these acid samples were taken for elemental analysis via the ICP-MS technique (inductively-coupled plasma/mass spectrometry).

The basic wipe samples (0.05 M NaOH) were processed quite differently. The absorbent paper was leached with a large excess (~15 ml) of 0.05 M NaOH and sonicated for approximately 10 minutes. The leachate was decanted off, and this procedure was repeated twice. The three leachates were then combined and centrifuged at 2000 rpm. The supernate from the centrifugation was transferred to a 50-ml class "A" volumetric flask and diluted to the mark with 0.05 M NaOH. Aliquots from these basic samples were taken for tritium analysis and for the inorganic analysis of a variety of anionic species by ion chromatography.

Tritium Analyses

The formation of tritium (^3H or T) in "cold fusion" cells has been taken as evidence of nuclear processes in the past. However, the deuterated or "heavy" water (D_2O) utilized in electrochemistry experiments around the world has frequently been contaminated with minute quantities of DTO. The detection of T in "cold fusion" work has consequently become unpersuasive as an indication of nuclear events. Nevertheless, LLNL routinely performs state-of-the-art T

measurements, and the SRI debris was interrogated for this nuclide as a matter of course.

A 5.0-ml aliquot of each of the basic-wipe samples (four debris specimens and one blank) was taken for T analysis by liquid scintillation counting (LSC). The 5.0-ml aqueous fraction was combined with 10 ml of Ultima-Gold XR reagent to form a LSC cocktail, and the five samples were then counted for 250 minutes each on a Beckman 9800 liquid scintillation counter.

None of the debris samples returned a counting rate above the LSC limit of sensitivity, nor did the process blank. The calculated LSC detection limit for T activity in these samples was 1.7 pCi/ml. Thus, no evidence for the presence of T was detected in the explosion debris that was examined by LLNL.

ICP-MS Analyses

Aliquots of each of the acid-wipe samples (four debris specimens and one process blank) were diluted by a factor of 10 and assayed via ICP-MS. The instrument was a VG PlasmaQuad Model PQ1 utilizing an argon plasma source, quadrupole mass-spectral separation, and an electron multiplier detector. Spectra were acquired over the entire periodic table of naturally-occuring elements, between masses 5 and 240, with sensitivities on the order of nanograms of analyte per ml of original solution (ng/ml or ppb). The chemical elements difficult or impossible to analyze by this technique were Na, Mg, Si, P, S, K, Ca, Fe, and Se.

The results of the ICP-MS analyses are presented in the following table, and a representative spectrum (of the wipe of the SS cell vessel wall) is depicted in the accompanying figure. The estimated concentrations of various analytes measured by ICP-MS were determined by comparison to a 50 ppb praseodymium internal standard added to each sample, with additional adjustments made to reflect differences in instrument sensitivity in different mass regions. The values in the table are semi-quantitative at best. However, due to the somewhat subjective nature of the wipe sampling, as well as to the fact that no normalization for differing sample surface areas was attempted, the ICP-MS results must be considered qualitative only.

Definite conclusions are possible from the ICP-MS results. Relative to the blank, all of the debris samples were enriched in traces of Li, Ag, and Pt. Selected debris specimens also indicated the presence of trace Mo, Pd, and Cd. In addition, the wipe of the SS cell vessel wall (SRI-2) showed evidence of

ICP-MS Results

Estimated Concentrations in ng/ml (ppb)

Sample	Li	B	Al	Ti	Mn	Ni	Cu	Zn	Sr	Zr	Mo	Pd	Ag	Cd	Sn	Ba	W	Pt	Pb	Bi	U
SRI-5 (blank)	DATA IN THIS TABLE CONSIDERED PROPRIETARY INFORMATION BY SRI INTERNATIONAL																				
SRI-1 (tef. cap)																					
SRI-3 (det. base)																					
SRI-4 (tef. liner)																					
SRI-2 (cell vessel)																					

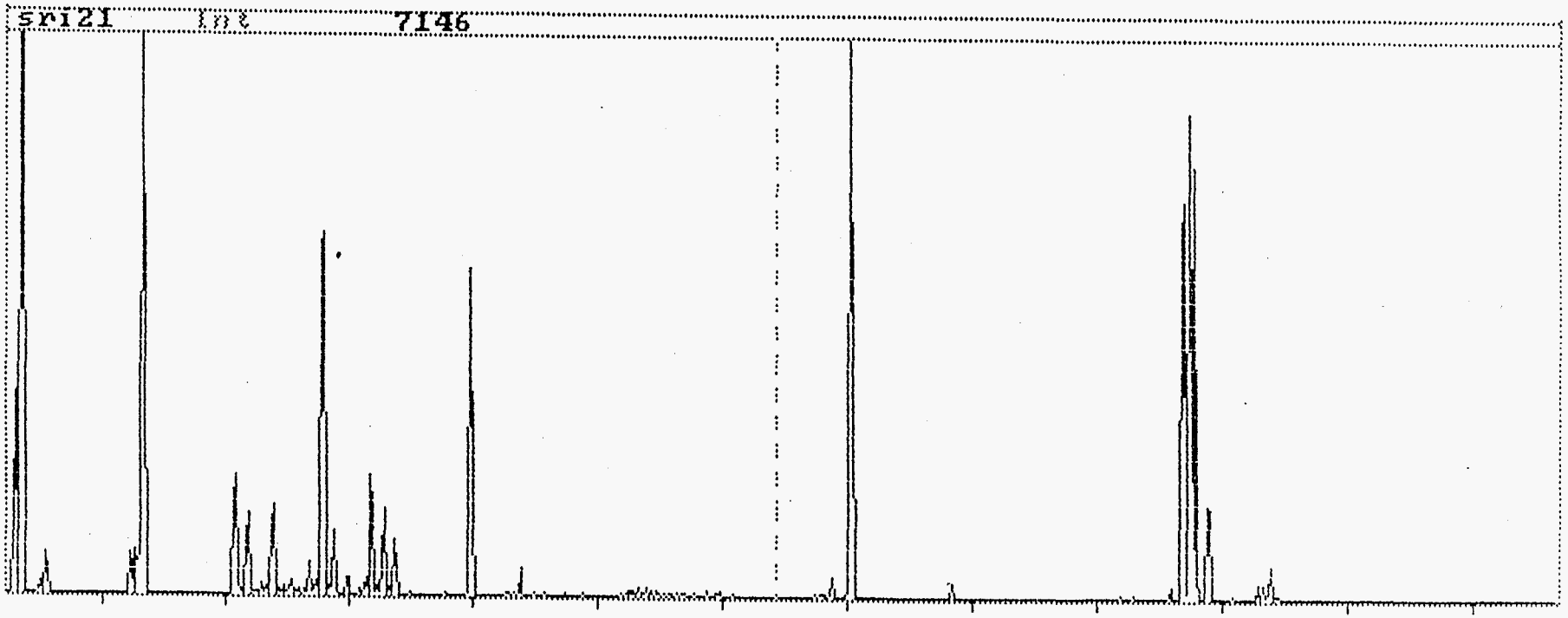
sri21
7146

elevated Al and Fe. [Fe is not listed in the data table because quantitative analysis of this element is hindered by interference from the ArO^+ molecular ion originating in the plasma torch; minor Fe mass peaks were definitely observed in sample SRI-2, however.]

In the normal operation of "cold fusion" electrochemical cells, materials incorporating Li, Pd, and Pt are expected. Fe, of course, is an unremarkable component of SS, and Mo is a minor component of the same material (ICP-MS evidence for Mo was limited to the metal debris specimens). The source of the Ag in the SRI debris was likely a silvered glass Dewar known to be surrounding the cell in its experimental configuration. This Dewar was shattered by the explosion.

Ion Chromatography Analyses

Suitable aliquots of each of the basic-wipe samples (four debris specimens and one blank) were taken for an ion-chromatographic investigation of the possible presence of unusual inorganic anions. The ions investigated were F^-, Cl^-, Br^-, NO_3^-, NO_2^-, $HPO_4^=$, and $SO_4^=$, and the instrument employed was a Dionex Model 2110i Ion Chromatograph with conductivity detection. The analytical column was an anion separation column Model AS4A, which was used in tandem with a conductivity suppressor column and 25 mN H_2SO_4 regenerant. Reagent eluants utilized for the separations were 2.5 mM $Na_2B_4O_7$ for F^- and Cl^-, and 1.7 mM $NaHCO_3$ - 1.8 mM $NaCO_3$ buffer for the rest of the anions.

Although F^- was not detected in the blank, it was measured in all of the debris samples except SRI-3, the detached cell base. The highest measured F^- concentration was 16 μg/ml(ppm) in the wipe solution from the cell interior (SRI-2), but the comments regarding the subjective nature of the sampling and the unequal sample surface areas mentioned in the ICP-MS section also hold for these ion chromatography results. The ubiquity of fluoride on the debris specimens is not surprising in light of the large quantity of Teflon present in the interior of the electrochemical cell.

Nitrate (NO_3^-) was slightly elevated in the SRI debris relative to the blank, but not by significant amounts (the maximum measured nitrate concentration was approximately 0.6 ppm). Nitrite (NO_2^-) results were below the limit-of-detection for that analyte (~0.1 ppm) in all samples. The absence of nitrate and nitrite in the explosion debris is noteworthy because they are inorganic residues often present in the aftermath of certain conventional explosions.

Conclusions

Inorganic chemistry results for tritium were negative, and atomic analyses by ICP-MS did not indicate the presence of any unusual elements that would not be expected in a normal experimental configuration of a "cold fusion" electrochemical cell. Inorganic speciation analyses by ion chromatography likewise proved negative for signatures of conventional explosives. Thus, the inorganic analytical results afforded no indication of a nuclear involvement, nor did they provide evidence for the presence of any unusual compounds suggestive of explosives, accelerants, propellants, or other exceptional industrial chemicals.

ORGANIC

ORGANIC CHEMISTRY ANALYSES AND RESULTS

Preliminary Comments

The purpose of these analyses was to search for any unusual organic species that might be present in the debris. Although not expected from what is presently known about this incident, LLNL easily and routinely interrogates diverse samples for residual evidence of propellants or conventional explosive signatures. These tests are extremely sensitive and were conducted here for completeness of the overall analysis.

In order to determine what trace organic compounds may have been present on the interior of the SRI explosion debris, selected components were extracted with wipes saturated with organic solvent. The organic species were then removed, concentrated, and analyzed by computer-guided gas chromatography-mass spectrometry (GC-MS). The results of those analyses are presented here.

Sample Pretreatment

The portions of the SRI debris specimens that were described in the Sampling Methods section of this report were extracted for possible trace organic species via the following protocols.

1. Absorbent Paper for Wipe Samples
   Cellulose papers (Whatman No. 4, ash-free) were folded and clamped with forceps. The paper was immersed in a clean solvent system of methylene chloride/isopropanol (3:1, Fisher Scientific, Optima Solvents) and extracted three times with fresh, clean solvent to remove most of the background organic contaminants in the paper. The final rinse with the extraction solvent rendered the paper suitable for sampling the interiors of the SRI debris specimens. A separate, pre-cleaned paper was used to extract the trace organic species from each debris component of interest.

2. Organic Extraction
   The selected area of each debris specimen was wiped with one pre-cleaned paper. Following each wipe, the extraction paper was soaked in a 10-ml vial containing 5 ml of methylene chloride/isopropanol solvent and squeezed semi-dry. This process was then repeated at a new location on the specimen surface. The final wipe was again soaked in the same 5 ml of solvent, squeezed dry, and the paper was archived for later analysis.

3. Concentration of Organic Extract

   The 5-ml solvent volume from each of the extractions was next evaporated under a stream of ultrapure nitrogen to a 10-µl concentrate. From this concentrated sample, an aliquot of 1.0 µl was then analyzed by GC-MS.

Gas Chromatography-Mass Spectrometry Analyses

The analysis of each of the samples utilized computer-guided GC-MS techniques for the separation and identification of all organic compounds extracted by the wipe sampling. Our laboratory employs fused-silica capillary columns, 30 meters in length, for component separation, and a Finnigan ion-trap mass spectrometer (ITMS) for the identification of all compounds eluted during analysis. Capillary columns provide very high separation factors for the various organic analytes of interest. The mass spectrometer then allows each of the separated species to be analyzed for molecular weight and structure, and this technique returns very detailed information about the chemical composition of the various samples.

The chromatograms included at the end of this section of the report depict the relative concentrations of various eluted compounds (y-axis) as a function of chromatography retention-time (x-axis). Typically, the larger and/or more polar the analyte compound, the longer the retention-time observed.

The results of the GC-MS analyses are summarized below. All of the samples tested positive for some residual organic matter. The identification of each individual compound was made through a computerized library search with comparisons to known compounds, as well as by individual interpretations of mass-spectral data.

1. Procedural Blank (Sample SRI-5)

   See the first attached chromatogram. The elution of extraction solvent during a GC-MS separation typically occurred over an interval of approximately 3 to 7 minutes after sample injection. The slight rise in the chromatogram baseline from 31-35 minutes is attributed to column bleed. This is a common feature of GC analyses due to the release of small amounts of stationary phase from the interior wall of long capillary columns during the end of temperature-programmed runs (typically reaching 250°C).

The total ionization plot of the concentrated sample obtained from the procedural blank (solvent saturation of Whatman No. 4 paper) revealed as the major component a long-chain olefinic compound eluting at 29.2 minutes after the start of the GC-MS run. This impurity was likewise observed in the majority of the wipe samples. A minor hydrocarbon peak was also seen at 23.2 minutes. The procedural blank was judged acceptable as a result of these GC-MS results.

2. Ripped Teflon Liner Wipe Sample (SRI-4)
   The interior of the Teflon liner revealed a series of silicones, phthalates, and short-chain hydrocarbons. Dioctylphthalate was the major compound isolated from the surface of the Teflon. The other compounds identified were tetramethylsiloxanes and other methyl-substituted siloxanes.

3. Detached-Base Wipe Sample (SRI-3)
   The detached stainless steel base was found to be coated with similar silicones and plasticizers. Dioctylphthalate was again the major compound on the surface of this debris specimen. No other major components were seen.

4. Teflon End-Piece Wipe Sample (SRI-1)
   The cap of the reaction cell contained a solid piece of Teflon. The wipe sample revealed the background olefinic impurity, as well as silicones and dibutylphthalate. No other unusual species were seen.

5. SS Cell Vessel Wall Wipe Sample (SRI-2)
   The surface area sampled with this wipe was estimated to be approximately 80 cm^2. This sampling of the metal walls of the electrolysis cell produced a chromatogram which identified silicones, dibutylphthalate, dioctylphthalate, and a series of compounds which were similar to organic oil.

   The chromatographic signature of the oil was indicated by the rise in baseline starting at a retention-time of 25 minutes and continuing on to 35 minutes after injection. Examination of the mass-spectral data over this time period revealed a continuum of hydrocarbon compounds, similar to that of saturated oil residues. Fragment ions at mass-to-charge ratios (m/z) of 57, 71, 85, 99, etc. were indicative of hydrocarbons. The appearance of these species, along with the characteristic chromatographic profile at elevated temperature (long retention times), is consistent with the presence of oil.

Conclusions

All of the wipe samples of the SRI debris contained trace amounts of organic contaminants. Compounds such as silicones and phthalates were identified in these samples, and such species are very common in the normal environment. The plasticizers are almost always associated with commercial plastics. The bags in which the specimens were stored could have been a likely source of these phthalates, as might reagent bottles used to initially contain reactant materials utilized in "cold fusion" experimentation.

The source of the silicones could have been the cell's internal o-ring or perhaps a silicone grease used to lubricate the o-ring prior to sealing the reaction vessel. Like plasticizers, silicones are found on nearly all industrial materials and are utilized for a variety of purposes, such as antifoaming agents and lubricants.

Mass-spectral data and GC-profile information strongly suggest the presence of organic oil on the walls of the metal reaction vessel. Similar hydrocarbon oil was not detected on any of the other debris specimens that were wiped. The GC-MS profile of the oil present on the cell vessel wall was indicative of a heavy oil, and not a kerosene or diesel-type fuel oil with high or medium volatility, respectively. The instrumental limit-of-detection for this oil was assessed to be on the order of ng for the wipe area of ~80 cm^2. However, analytical experience in the processing of similar oil samples led to an estimate of hundreds of μg of oil in the subject debris wipe. In evaluating these data, it should be remembered that the wipe sampling interrogated only a fraction of the interior surface of the steel cell and that sampling occurred after an explosion of considerable force.

Supplementary Remarks

The presence of silicones, phthalates, and short-chain hydrocarbons in the debris is not unusual. Nearly all materials either contain these compounds, or are coated with such lubricants and plasticizers; appropriate cleaning of ordinary items with suitable, ultraclean solvents in order to remove all traces of organic residues is rarely performed. No organic explosives, oxidizers, or other unusual compounds associated with more conventional explosions were detected in the SRI debris samples.

The oil identified in the interior of the electrolytic cell may have originated from the fabrication of the metal container. Much hydrocarbon oil is often

utilized during machining to cut threads, drill holes, turn on a lathe, and fabricate most metal parts.

We cannot absolutely guarantee that the detected oil was a component of the "cold fusion" reaction mixture at the time of the explosion. The debris was extensively handled by several organizations after the incident in a fashion largely unknown to us. It is possible that the oil was introduced as an external contaminant during the 3.5 months between the explosion and receipt of the evidence by LLNL. However, none of the other sampled specimens tested positive for this analyte, and the interior of the steel cell was more protected from potential environmental influences than the rest of the debris. Moreover, the GC-MS analyses were also very sensitive to the presence of palmitic acid, stearic acid, and cholesterol. The former two compounds are signature species for fingerprint residues and common human handling, while the latter is a general indicator of biologic contamination. None of these particular indicator compounds were detected in any of the GC-MS analyses.

Organic oil in the interior of an electrochemical "cold fusion" cell may be quite important. The reaction mechanism of "cold fusion" involves the electrolytic decomposition of D_2O to form overpressures of gaseous D_2 and O_2. As the D_2 is sorbed into the matrix of a Pd electrode, the cell headspace presumably becomes enriched in O_2. Hydrocarbons are an excellent fuel for combustion with oxygen. In fact, some bipropellant rocket fuels utilize only oxygen and a hydrocarbon source (kerosene) as the propulsion system. Some types of propellant systems are described as hypergolic, meaning that they self-ignite on contact between the fuel and oxidizer.

A well-known problem in the manufacture of rocket engines is the instability generated when oxygen is exposed to organic residues. Pure oxygen, in contact with the carbon source, can react violently with very small amounts of organic material (e.g., residues of oil or grease). Furthermore, with a stimulus of pressure, shock, heat, etc., a violent secondary reaction between the oxygen and a metal container can also occur.

If oil residue is present in the interior of a "cold fusion" reaction cell when overpressures of oxygen are generated during electrolysis, there is a distinct possibility that an exothermic, explosive reaction could take place. The utilization of organic residues (including silicones and phthalates) as a combustion source is quite credible.

An important protocol in the high-pressure gas community is that any components in an oxygen atmosphere must be scrupulously cleaned to avoid explosions and catastrophic overpressures caused by heat from the combustion of organic residues. The American Society for Testing and Materials (ASTM) requires clean-room conditions and decontamination procedures for any oxygen containment components. All equipment utilized for oxygen service, whether the oxygen is a component of a mixture or present as a pure gas, must be specifically cleaned to remove any traces of oils, greases, or other hydrocarbon materials. Procedures for cleaning components and systems to be used for oxygen containment have been clearly outlined in the third edition of **The Handbook of Compressed Gases.** A direct quote from this reference reads, *"Caution: Never permit oil, grease, or other combustible substances to come in contact with cylinders, valves, regulators, gases, hose, and fittings used for oxidizing gases, such as oxygen and nitrous oxide, which may combine with these substances with explosive violence."*

In conclusion, it would be prudent to establish effective cleaning procedures for hydrocarbon impurities likely to be present on apparatus utilized in the interior of "cold fusion" electrochemical cells. Such measures should be relatively unobtrusive in the design and practice of such experiments.

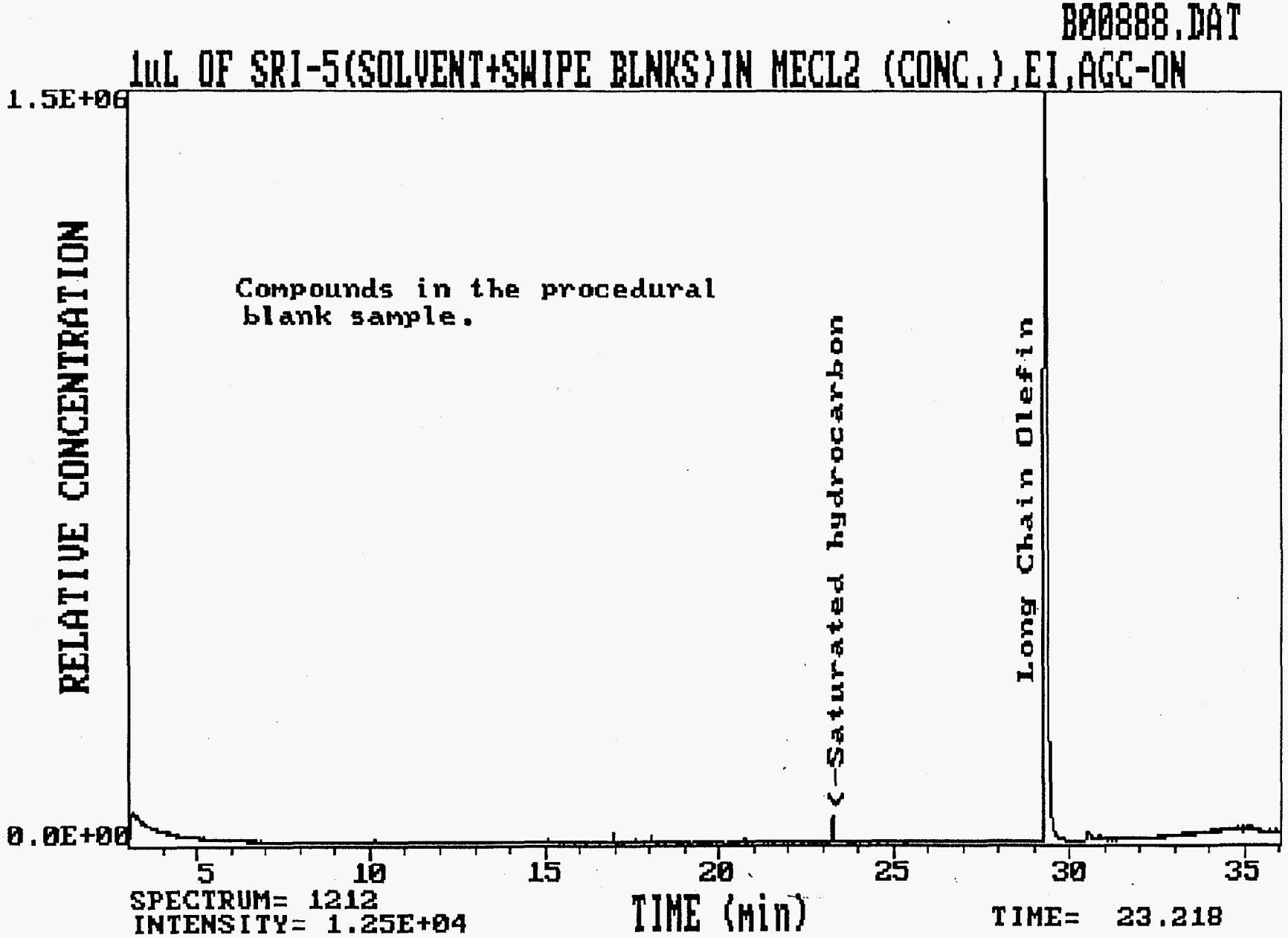
B00888.DAT
1uL OF SRI-5(SOLVENT+SWIPE BLNKS)IN MECL2 (CONC.),EI,AGC-ON
1.5E+06
0.0E+00
RELATIVE CONCENTRATION
Compounds in the procedural blank sample.
C-Saturated hydrocarbon
Long Chain Olefin
5
10
15
20
25
30
35
TIME (min)
SPECTRUM= 1212
INTENSITY= 1.25E+04
TIME= 23.218

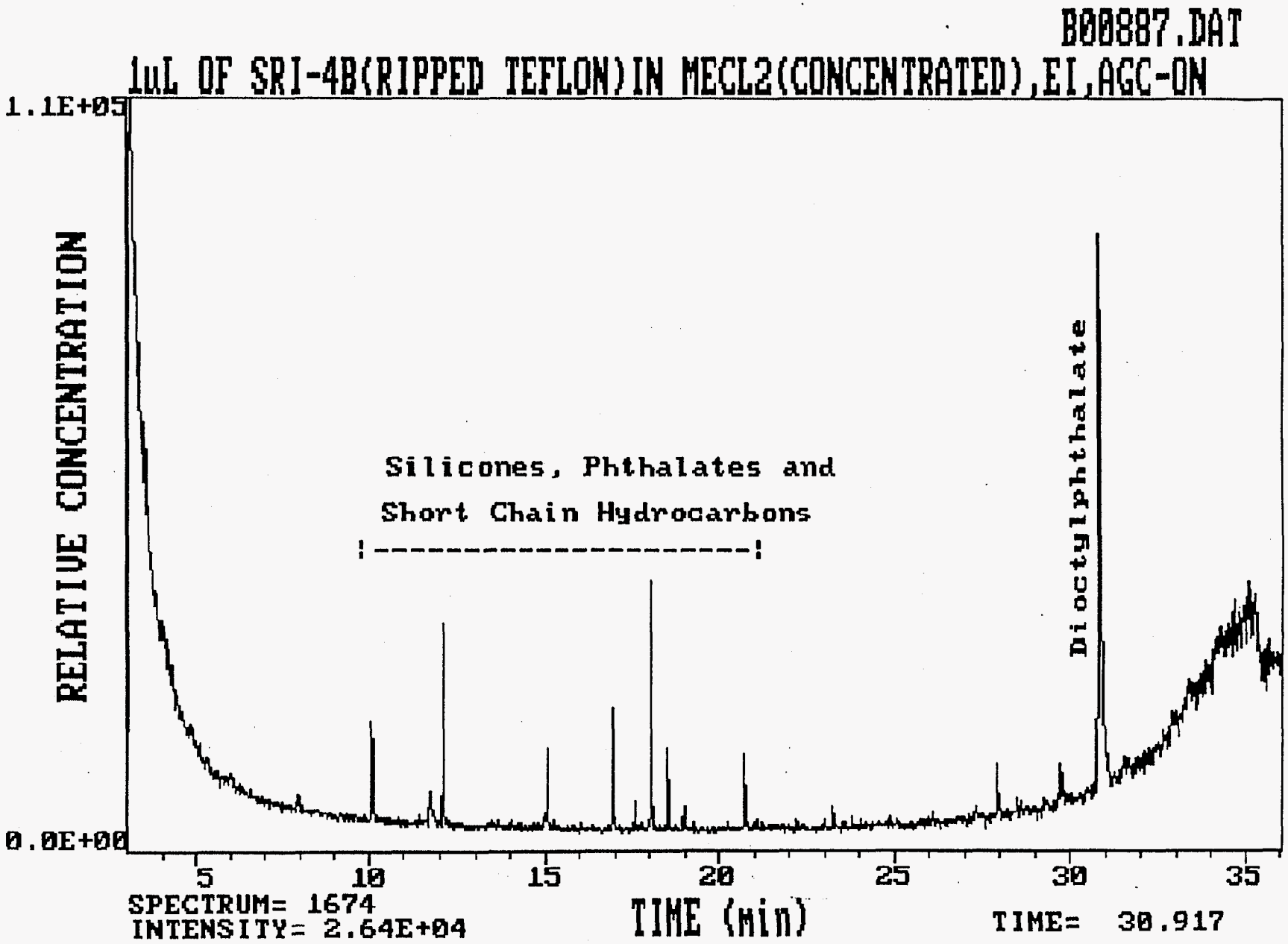
B00887.DAT
1uL OF SRI-4B(RIPPED TEFLON)IN MECL2(CONCENTRATED),EI,AGC-ON
1.1E+05
0.0E+00
RELATIVE CONCENTRATION
Silicones, Phthalates and
Short Chain Hydrocarbons
Dioctylphthalate
5
10
15
20
25
30
35
TIME (min)
SPECTRUM= 1674
INTENSITY= 2.64E+04
TIME= 30.917

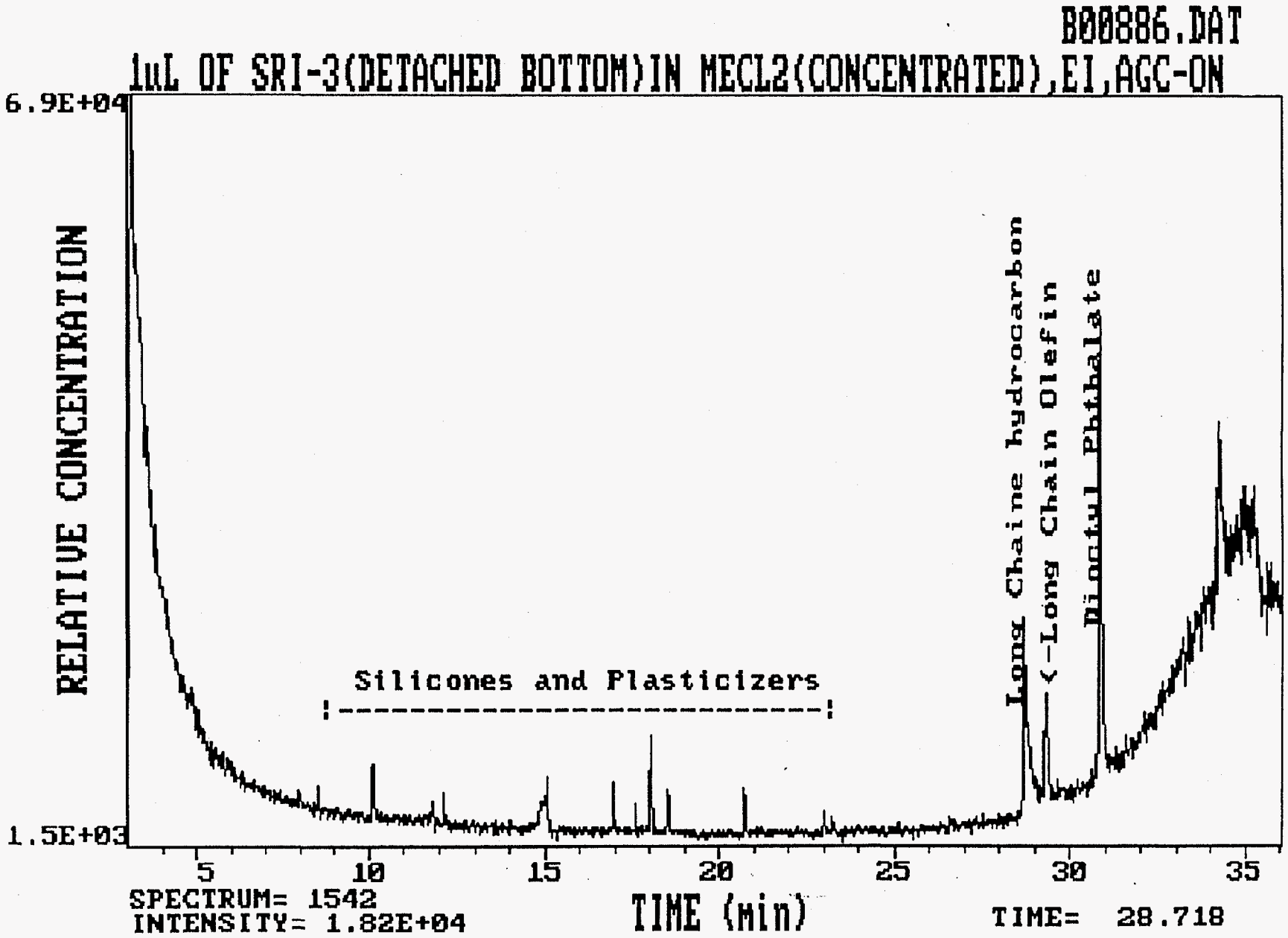
B00886.DAT
1uL OF SRI-3(DETACHED BOTTOM)IN MECL2(CONCENTRATED),EI,AGC-ON
6.9E+04
1.5E+03
RELATIVE CONCENTRATION
Silicones and Plasticizers
Long Chaine hydrocarbon
<-Long Chain Olefin
Dioctyl Phthalate
5
10
15
20
25
30
35
TIME (min)
SPECTRUM= 1542
INTENSITY= 1.82E+04
TIME= 28.718

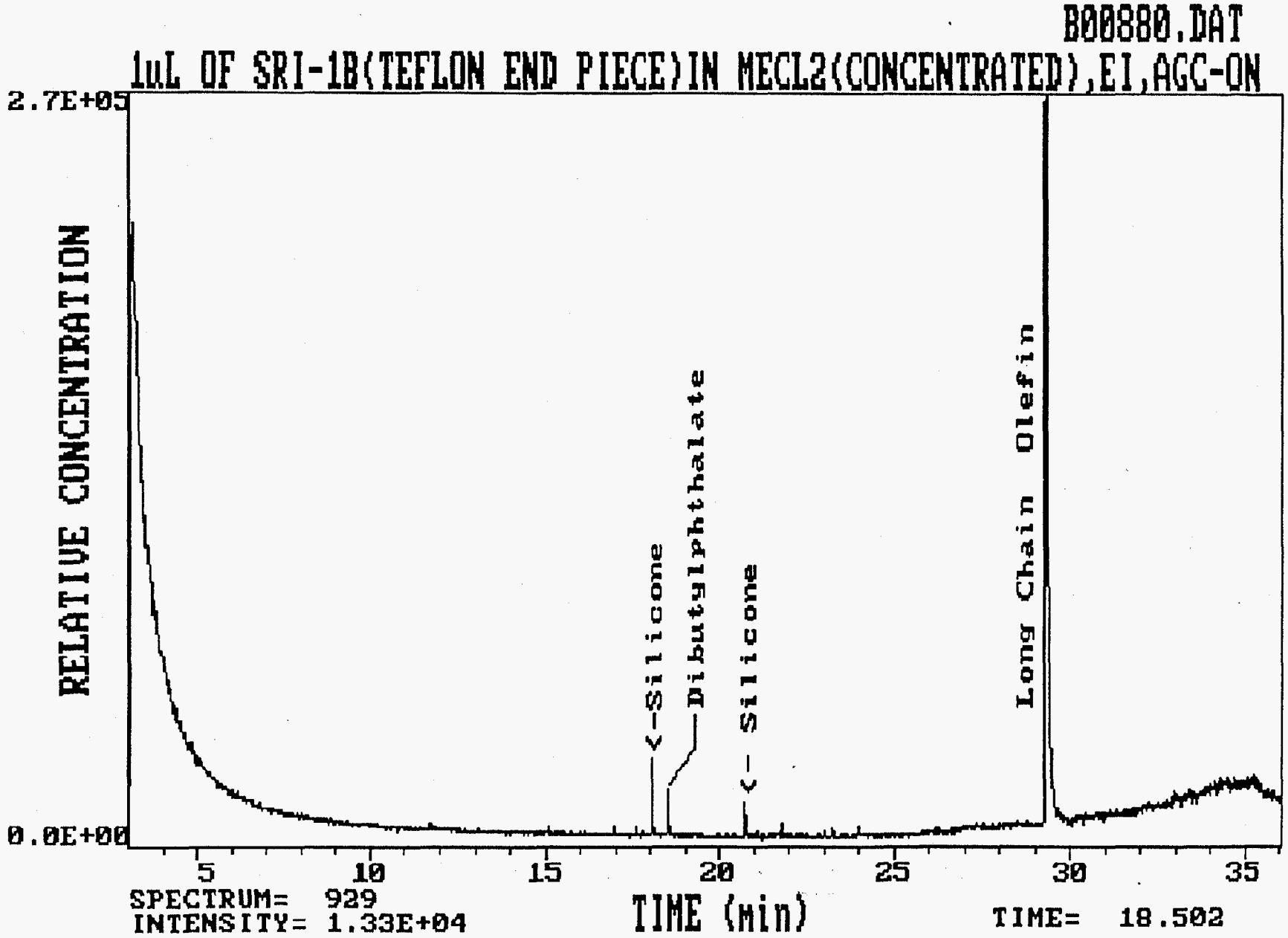
B00880.DAT
1uL OF SRI-1B(TEFLON END PIECE)IN MECL2(CONCENTRATED),EI,AGC-ON
2.7E+05
0.0E+00
RELATIVE CONCENTRATION
<-Silicone
Dibutylphthalate
<- Silicone
Long Chain Olefin
5
10
15
20
25
30
35
SPECTRUM= 929
INTENSITY= 1.33E+04
TIME (min)
TIME= 18.502

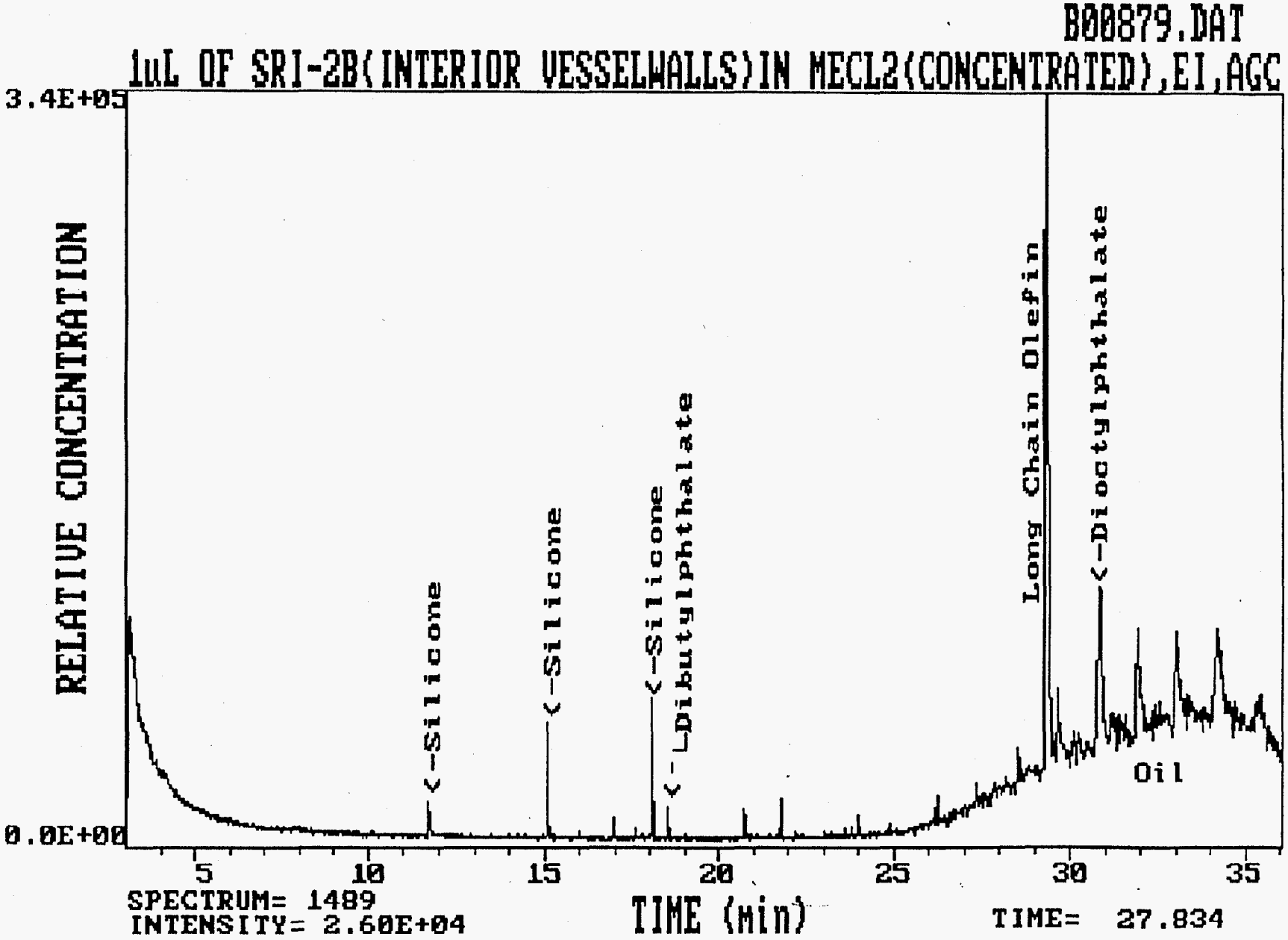
B00879.DAT
1uL OF SRI-2B(INTERIOR VESSELWALLS)IN MECL2(CONCENTRATED),EI,AGC
3.4E+05
0.0E+00
RELATIVE CONCENTRATION
<-Silicone
<-Silicone
<-Silicone
<-Dibutylphthalate
Long Chain Olefin
<-Dioctylphthalate
Oil
5
10
15
20
25
30
35
TIME (min)
SPECTRUM= 1489
INTENSITY= 2.60E+04
TIME= 27.834

PARTICULATES

PARTICULATE ANALYSES

Preliminary Comments

The quantity of solid material recovered from the interior walls of the electrochemical cell and the detached base was miniscule and was estimated to weigh perhaps a total of a few hundred micrograms. Such small mass precluded most conventional nondestructive analytical techniques for the chemical study of solid samples (e.g., quantitative x-ray fluorescence spectroscopy). However, LLNL is capable of performing sensitive analyses of individual particulate samples as small as a few microns in length. These analyses provide information on elemental concentrations, oxidation states, and isotopic compositions of an individual particle specimen.

Debris particles recovered from the stainless-steel cell vessel were analyzed separately from those scraped from the detached cell base. The techniques used were ion microprobe mass spectrometry (IMMS), scanning electron-probe microanalysis (SEM), and electron spectroscopy for chemical analysis (ESCA).

Electron and Ion Microprobe Analyses

Distinct white, black, and brownish particles were selected from the sampling of the cell interior for analyses by IMMS and SEM. The more homogenous white particles from the cell base were analyzed as a single population by these same instrumental techniques. A total of seven particulate specimens were taken for these studies, and their composite weight was estimated at ~200 μg. The total quantity of material consumed by these techniques was ~240 ng; the remainder will be preserved for archival purposes.

A copy of detailed summaries of the IMMS and SEM analyses are provided at the end of this section of the report. The black and brown particulates from the cell interior were identified as consisting fundamentally of an Al_2O_3 matrix with 10-μm subhedral inclusions of Pt interspersed throughout. The white particles from both the cell interior and the detached cell base were characterized as LiOH + LiOD.

Although isotopic analysis of D/H in these latter specimens revealed enrichment factors of 80-180 relative to normal samples, an initial puzzle was that the most enriched sample that we analyzed still contained 40 times more protons than deuterium atoms. For electrochemical experiments at high

concentrations of LiOD in reasonably pure D_2O, one might expect very much higher D/H ratios in the residual LiOD than those actually measured.

A plausible explanation for this finding is isotopic exchange between LiOD and H_2O in normal atmospheric water vapor over the five months since the initial explosion. LiOH-LiOD is known to readily absorb water from the air, and no attempt after the incident was made to isolate the small and finely-divided quantitiy of residual LiOD from subtle environmental interactions. The loss of deuterium enrichment through free exchange with atmospheric H_2O of normal isotopic composition is consistent with what is presently known about exchange equilibria in the H/D isotopic system.

ESCA Analyses

The remainder of the particulate specimens that were not utilized for IMMS and SEM were taken for ESCA. They were adhered to small pieces of carbon tape and mounted on posts in order to concentrate them into as small an area as possible. However, the amounts of sample available from both the cell-interior and detached-base locations were so small as to present a serious challenge for composition determinations by the ESCA technique.

The interrogation of both specimens over a suitable surface area was performed with a Perkin-Elmer 5400 ESCA system via x-ray photoelectron spectroscopy. An extremely long (~14 hours), broad scan was taken to identify the elemental composition of each sample with maximum sensitivity. This initial scan was then followed by high-resolution scans to measure atomic concentrations and effect oxidation-state analyses. Speciation determinations by ESCA are accomplished by means of regression analysis at appropriate regions in the photoelectron spectrum.

The elements identified in the residue from the detached cell base by ESCA were Si, O, Li, and Mg, with the Si present as the R-Si-O functional group (102-eV binding energy). The ESCA sample from the interior of the SS cell was a mixture of black and white particles. The elements present at highest concentration in this sample were C, O, Li, Al, and F, and all were measured at levels greater than 2 atomic percent (Li was present at 13 atomic percent). Alumuinum was characterized as Al_2O_3 and Si again as R-Si-O. Approximately 10% of the assayed carbon was identified as $-CF_2$ (the Teflon polymer chain). The Li binding energy of 55.5 eV was tentatively ascribed to LiF; however, LiOD could not be ruled out as the actual chemical form of the Li because the ESCA spectrometer was not calibrated for that particular species.

None of the ESCA results were surprising when considered in light of the ususal reagents and materials expected in the normal operation of a "cold fusion" electrolytic cell. Considering the meager quantity of analyte and the more heterogeneous nature of the ESCA analytical samples, consistency of the ESCA results with the IMMS and SEM analyses was quite satisfactory.

Interdepartmental letterhead

Mail Station L- 237

Ext. 3-1968

June 1, 1992

TO: Pat Grant

FROM: Doug Phinney DP

SUBJECT: *Particles from a "Cold-Fusion" Cell: Ion-microscope Results*

On May 12, 1992, Pat Grant requested that the electron microprobe and the ion microscope in the LLNL Nuclear Chemistry Division be used to analyze two samples of granular material collected from a "cold-fusion" cell. On May 13, I selected seven submillimeter particles from these samples. The analyses of these particles were aimed at answering the following questions:

(1) Could the particles be identified with specific materials known to be in the cell when it was operating?

(2) Assuming such identifications could be achieved, what isotopic compositions and trace elements could be identified in the particles.

Particle Description and Preparation

The two samples were labelled **CELL INTERIOR** and **CELL BOTTOM.**

(1) Particles from CELL INTERIOR.

Five particles were removed from this sample. The following descriptions of these particles were obtained by examination in an optical microscope.

(a) White particles (labelled White I and White II). These particles are translucent, milky white. They are tabular (or "platy"); the "plate" thickness is ~100μm.

(b) Brown particles (labelled Brown I and Brown II). These particles are opaque and dark brown. The surfaces have a glassy (or "shiny") appearance. These particles appear to be clumps of ~100μm diameter grains, cemented together.

(c) Black particle (labelled Black I). This particle is opaque and dark gray. The surface has a matte finish and appears to be sintered.

Each CELL INTERIOR particle was mounted on an aluminum stub with conductive (silver-filled) epoxy. Each stub was cast in "ordinary" epoxy in a cylindrical ring form with the particle near one of the flat faces of the forms. Each form was sent to the Metallurgy Lab of the LLNL Chemistry and Materials Directorate, where it was polished until a cross-section of the particle was exposed. The polish was performed without water, and the final polish was achieved with 0.25 μm diamond compound. Bob Kershaw performed the polishing.

Mounts White I, Brown I, and Black I were coated with ~200 Å of carbon to form a conductive film on the "front" surfaces (i.e., on the surfaces where the particles were exposed). The back sides of these mounts were coated with ~1000 Å of gold, in order to provide a conductive path from the aluminum stub to the periphery of the mount.

(2) Particles from CELL BOTTOM.

Two particles were removed from this sample. These particles are translucent, milky white. They are friable and shed small (~1 to 10μm in diameter) crystals upon handling. Because of the friability, a different mounting procedure was used for these particles.

A plastic membrane with 18μm holes was coated with ~2000 Å of gold. The two particles were "smeared" onto the gold-coated membrane surface with the end of a glass stirring rod. The "smearing" process caused the particles to crumble, allowing some of the resulting crystals to stick in the 18μm holes. The bulk of the "smeared" crystals merely stuck to the gold between the 18μm holes. Then, the mount was coated with ~1000 Å of gold. This mount was labelled CELL BOTTOM.

Results

Mounts White I, Brown I, Black I, and CELL BOTTOM were analyzed with the ion microscope. Mounts Brown I and Black I were analyzed with the electron microprobe.

The electron-microprobe analyses showed that particles Brown I and Black I are similar in their major- and minor-element chemistry; namely, each is essentially Al_2O_3 with a minor amount of platinum. (See memo from Dave Smith.)

The ion-microprobe analyses consisted of four parts:

(1) Burn-in depth profile; resolving power ~300.

(2) Mass survey (after burn-in). This is a mass spectrum from mass 1 to 280 at a resolving power ~300.

(3) Ion-imaging of the dominant elements seen in the mass survey; resolving power ~300.

(4) Isotopic ratios of H, Li and B at resolving power ~1500. (A resolving power of 1300 is required to distinguish ^2H from H_2.)

The ion microscope was operated with a 12.5 kV $^{16}O^-$ sputtering beam, and the sputtered ions from the particles were analyzed as positively charged species. Under these conditions, detection limits are ~10 atomic parts per billion for most metallic ions and ~100 atomic parts per billion for H, O, C, and halogens.

Burn-in Results

All samples show a layer of trace-level surface contamination a few tenths of a micrometer thick. The contaminants comprise alkalis, alkaline earths, organics, and halogens. For mounts White I, Brown I and Black I, the burn-in profile removed the contaminant layer, and the subsequent ion-microscope measurements were made in the "meat" (as opposed to the surface-contaminated "skin") of the particles. The crystals of the CELL BOTTOM mount are so small that the surface contaminants remained at nearly full strength after the burn in.

The intensities of elements during the burn-in profile give a clear indication of the major elements for each mount. There are two groups of mounts on the basis of major elements.

(1) Brown I and Black I. Major elements are aluminum and oxygen.

(2) White I and CELL BOTTOM. Major elements are lithium, oxygen, and hydrogen.

Mass Survey

The mass surveys confirmed the grouping of Brown I and Black I and of White I and CELL BOTTOM. In other words, particles in a given group have similar mass spectra, and the mass spectra of the two groups differ markedly. The mass surveys of Brown I and Black I show the clear presence of platinum, albeit a minor constituent. It is worth noting that no evidence of palladium was seen in any of the mass spectra.

Imaging Results

Major-element images gave uniformally illuminated images with clear delineation of topographic features (e.g., cracks or grain boundaries). This was true of aluminum and oxygen for Brown I and Black I; whereas White I and CELL BOTTOM showed this behavior for lithium, hydrogen, and oxygen. Contaminant elements show patchy distributions of their images. The platinum images for Brown I and Black I occur as faint isolated "sparkles" and the intensity showed a spatial frequency of ~1 sparkling spot/300$(\mu m)^2$.

Isotopic-ratio Results

There is a spread of D/H ratios. The White I and CELL BOTTOM group has the higher D/H ratios.

Sample	D/H	Relative to normal D/H ratio
Brown I	0.0031	~20
Black I	0.00013	~1
White I	0.012	~80
CELL BOTTOM	0.027	~180
Normal D/H	0.00015	=1

It is worth noting that the ^1H atoms outnumber the ^2H atoms by ~30:1 in the most deuterium-enriched sample (CELL BOTTOM).

Isotopic ratios have an uncertainty of ~10%. This could be improved to a few tenths of a percent if there were time to analyze standards.

DP92/86

May 25, 1992

TO: Pat Grant

FR: D.K. Smith, L-232, x35793

RE: Microimaging and analysis - SRI Black Sample #1 and Brown Sample #1

Attached please find six photomicrographs and accompanying energy dispersive spectral (EDS) analysis for the Black #1 and Brown #1 SRI samples provided this week. As sent, the particulate samples were mounted on a conductive stub, the stub centered within a plastic ring and the entire assembly immersed in epoxy. After curing, sample surfaces were finished to a high polish (0.05 alumina); in the laboratory, I subsequently cleaned the polished surfaces with isopropyl alcohol and applied approximately 200 angstroms of carbon film prior to electron probe micro-analysis (EPMA).

SRI Black Sample #1

The three images represent magnifications of 180x, 400x and 800x; a micron scale bar appears along the side of each photograph. Each photomicrograph represents a backscattered electron image sensitive to mean atomic number. Regions of higher Z will be represented as lighter on a gray scale of black to white; as such, epoxy impregnated areas are black. The images clearly show an inherent internal porosity with void spaces up to and exceeding 10 microns in dimension. Texturally, the particle appears seemingly as a composite sinter; individual grains, some with internal porosity, range typically from 10 to 50 microns in maximum dimension. The backscattered gray scale imaging indicates only slight variations in composition throughout the surface. The few minute bright higher Z particles imaged around the edges of the particle in the 180x photomicrograph are surficial Ag flakes likely introduced by the conductive paint routinely used in grounding all EPMA samples; notably, no Ag flakes are observed within the particle's matrix .

In contrast to the images, EDS measurements represent 'spot' analyses of <1 micron diameter. These analyses are qualitative with peak height being only relatively correlated with abundance. Analysis of approximately 10 points throughout the matrix, including an array of contrasting grains as imaged, indicates the matrix is composed exclusively of aluminum. The second peak is either a trace Zr L alpha or overlapped Pt L alpha subsidiary. It should be noted that EDS is incapable of measuring elements lighter than F, hence oxides are represented by their cation equivalents only.

SRI Brown Sample #1

Photomicrographs were taken at magnifications of 120x, 600x and 800x with backscattered electrons. Texturally the matrix appears as equigranular composite with conspicuous grain boundaries and intergranular void space. Single grains range from 10 to 50 microns in

maximum dimension and appear without internal porosity. The uniform gray scale across the matrix indicates compositional homogeneity; notable however are small (10 micron) subhedral particles of high atomic number which appear interspersed irregularly throughout and internal to the matrix.

EDS analyses indicate the matrix to be aluminum. EDS analysis of the high Z particle imaged at 800x identifies Pt ; analysis of the high Z particle imaged at 600x identifies Pt and Cl.

Sample as prepared have been transferred to D. Phinney for trace element and isotopic profiling by secondary ion mass spectrometry (SIMS).

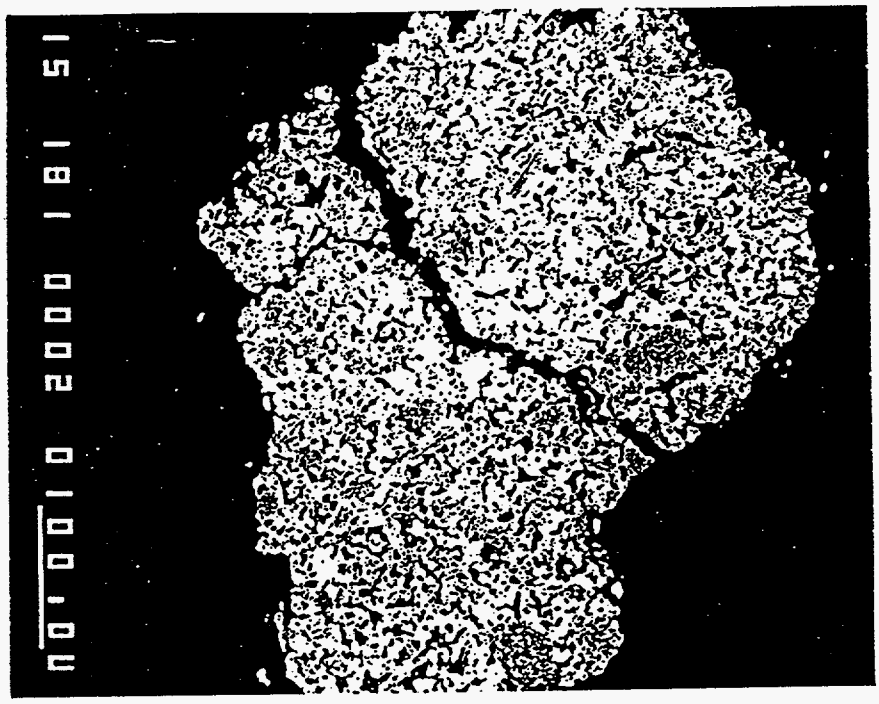

SRI Black Sample #1 180x

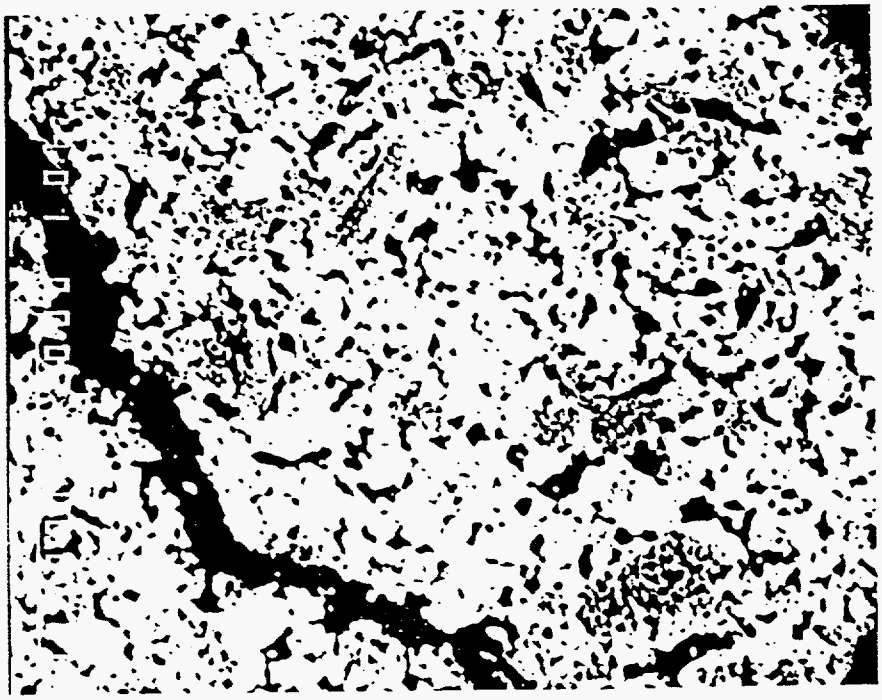

SRI Black Sample #1 400x

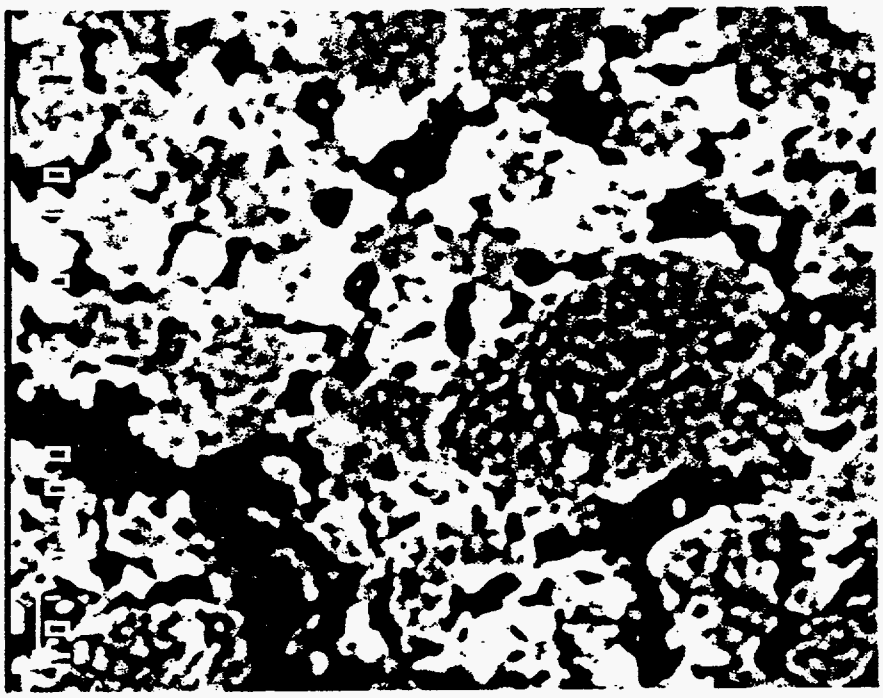

SRI Black Sample #1 800x

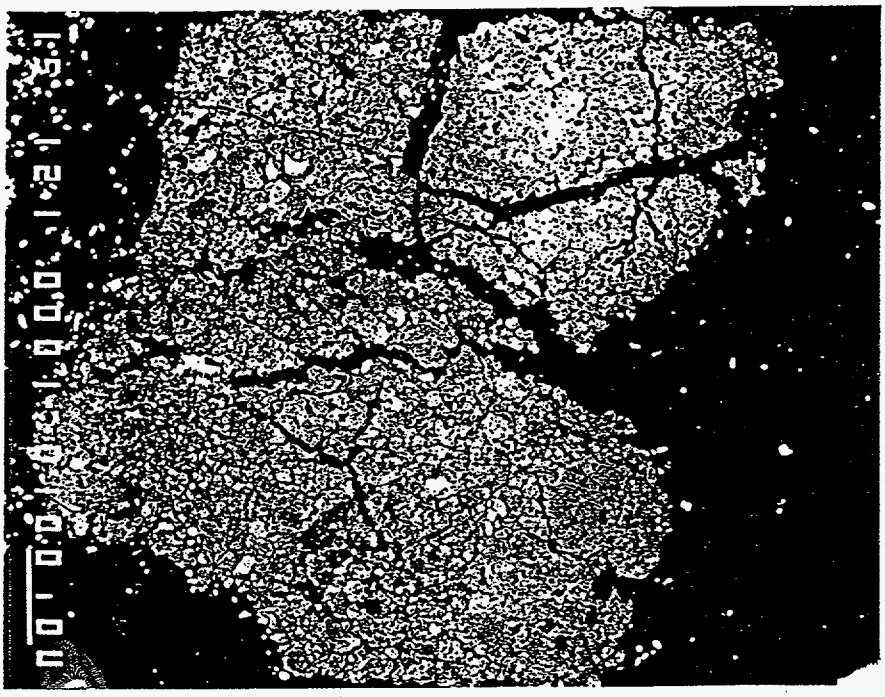

SRI Brown Sample #1 120x

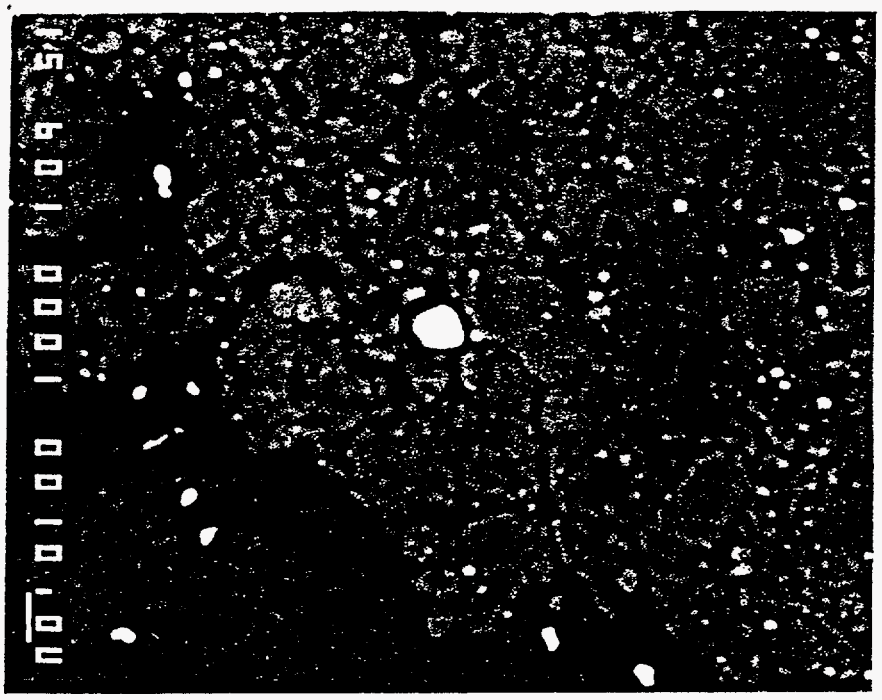

SRI Brown Sample #1 600x

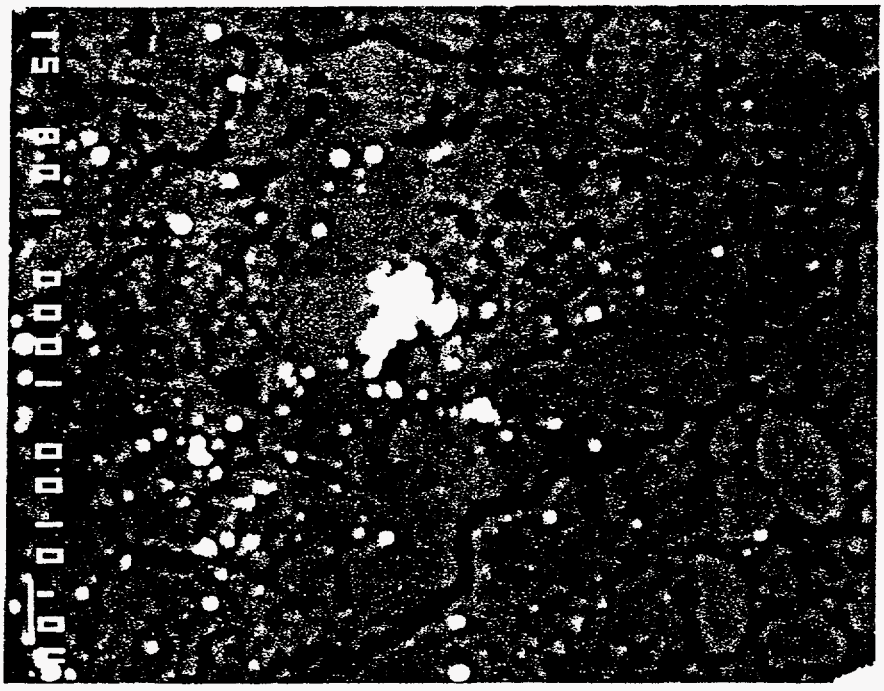

SRI Brown Sample #1 800x

TASK:

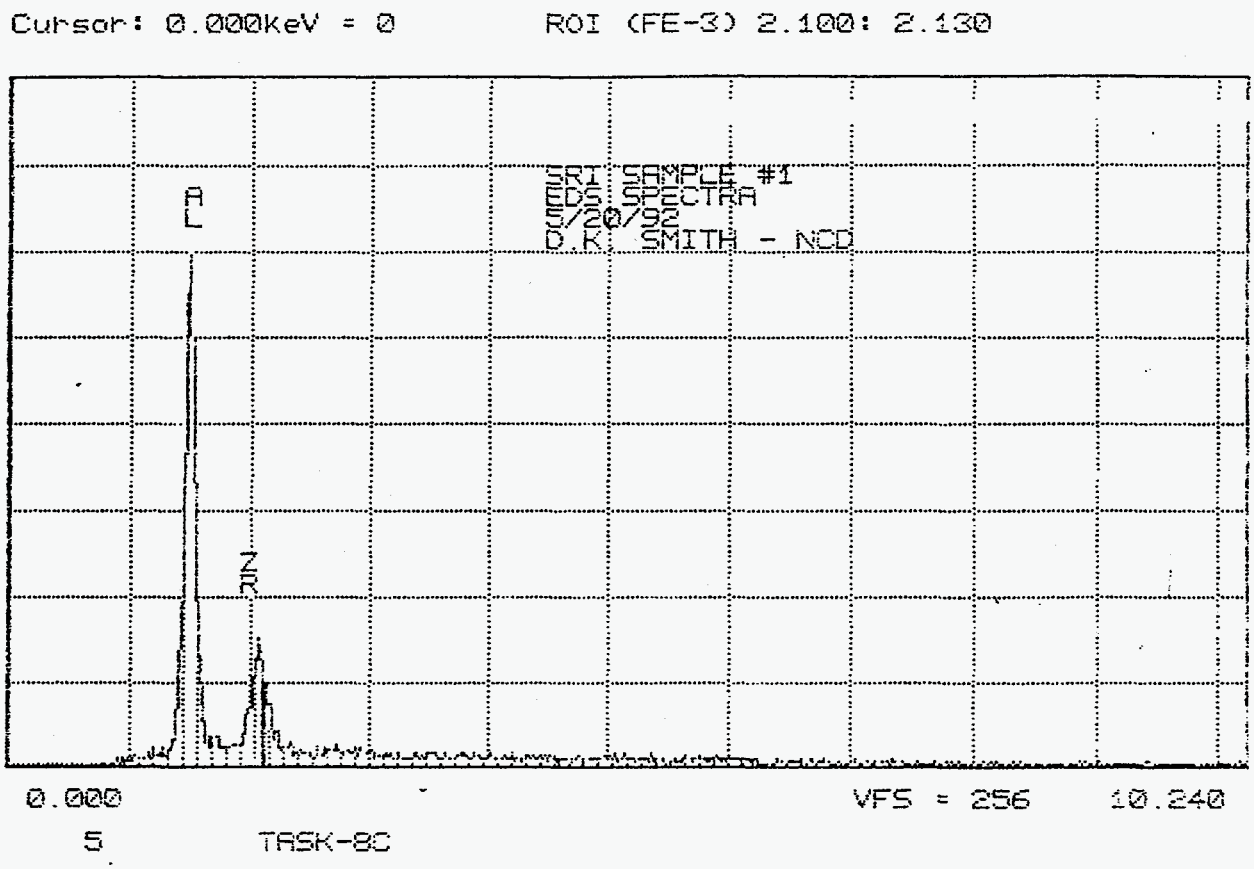

SRI Black Sample #1

TASK:

Lawrence Livermore National Labs FRI 22-MAY-92 16:12

Cursor: 0.000KeV = 0

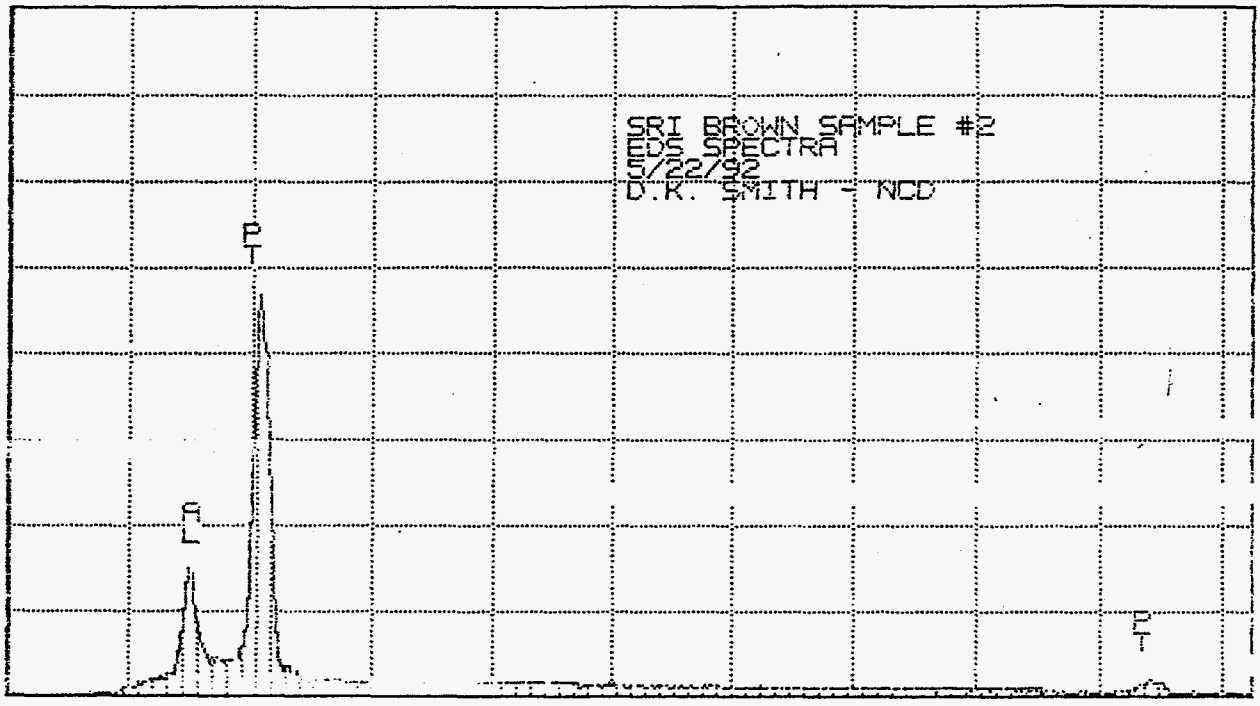

0.000 VFS = 2048 10.240

10 TASK-8C

SRI Brown Sample #1 800x

Lawrence Livermore National Labs FRI 22-MAY-92 16:29

Cursor: 0.000keV = 0

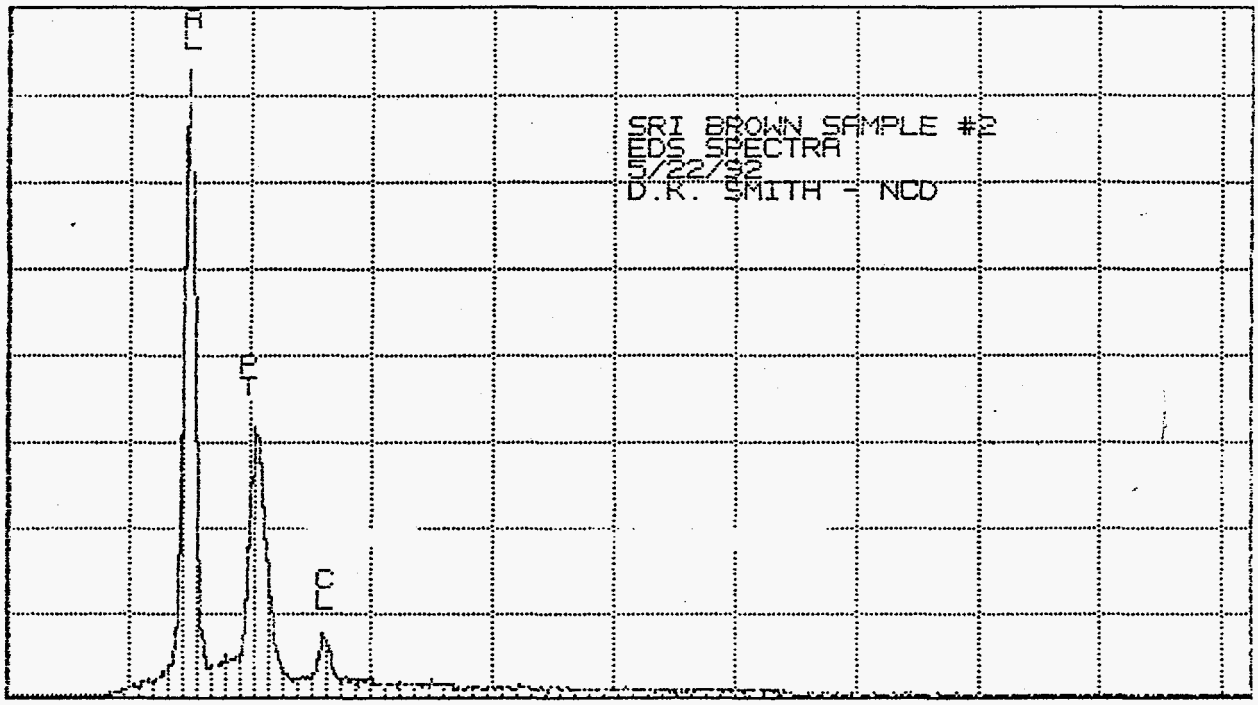

SRI Brown Sample #1 600x

MATERIALS & STRUCTURAL

MATERIALS CHARACTERIZATION AND STRUCTURAL ANALYSES

Nondestructive XRF Analyses

One of the main questions remaining at SRI following their analysis of this incident was the specific type of stainless steel (SS) utilized in the fabrication of this particular electrochemical cell. According to SRI's Fran Tanzella, the most likely choices were type 304 SS or type 316 SS. To answer this question, LLNL performed nondestructive x-ray fluorescence (XRF) spectroscopy on strategic portions of the SS cell vessel and the detached base. As type 316 has a significantly higher concentration of Mo in its composition than type 304, XRF analyses of Mo concentration were considered decisive for materials discrimination.

We used a Kevex Analyst Model 770 energy-dispersive XRF spectrometer with secondary-target fluorescence. The secondary target utilized for analyses of the cell debris was Ag, so that the effective elemental upper limit for the x-ray spectra was Rh. The SRI samples were analyzed at instrument settings of 50 keV and 0.2 mA, and peak identification and integration were performed with proprietary Kevex software and Gaussian deconvolution. Quantitative analysis was effected by comparison with National Institute of Standards and Technology (NIST; formerly the National Bureau of Standards [NBS]) primary SS standards. Computational tactics included the utilization of only K_α lines in the analyses and normalization of Mo values to the Cr compositions of the SS specimens.

XRF analyses of one type-304 NIST primary SS standard (SRM 1152) and two type-316 NIST primary SS standards (SRM 1155 and SRM 1185) were used for system calibration. The NIST-certified values for the weight-percent ratio of Cr to Mo [W(Cr/Mo)] in these standards are 50.5, 7.8, and 8.5, respectively. Thus, W(Cr/Mo) in type 304 SS is approximately a factor of six greater than W(Cr/Mo) in type 316 SS, and this measurement can serve as a basis for characterization.

Qualitative XRF results for the elements present at detectable levels in the SRI debris identified Cr, Mn, Fe, Co, Ni, Nb, and Mo in all samples. Determinations of W(Cr/Mo) in these specimens resulted in the following values: 8.4 for the detached base, 8.6 for the body of the cell vessel, 6.5 for the threaded cell cap at an undistinguished location, and 6.3 for the threaded cell cap at the location of the black smudge mark. The XRF data from this last position also indicated the presence of Cu and Zn in roughly the correct

proportions for metallic brass, and this was the only interrogated location that registered positive for these two metals.

Provided that the only choices are type 304 or type 316 SS, the XRF measurements indicated that the electrochemical cell was manufactured from type 316 SS. However, this analysis does not preclude the possibility of other Mo-rich stainless steels, such as types 316L or 317. XRF data also suggest that perhaps the cell impacted a brass object at the location of the black mark on the cell cap following the explosion. Alternatively, the brass component may reflect imbedded material from the heat-exchanger fins which surrounded the cell vessel at the time of the explosion.

High-Energy X-Ray Radiography

Before disassembly of the threaded-cap structure from the SS vessel wall, the interiors of the electrochemistry cell and the gas tube were imaged by means of a Varian industrial radiography instrument. This machine is an electron linear accelerator with continuous energy variability up to 9 MeV, and high-energy x-radiation is produced as bremsstrahlung in a tungsten target.

Two x-ray energies were employed for the interrogation of the SRI cell. A lower energy (200-keV) beam was used for higher resolution within the gas tube, while high-energy (4-MeV) x-rays were utilized for better detail inside the thicker SS walls. A copy of the detailed radiography report is included in the immediately-following pages.

Also included here are glossy prints of three selected radiographs. Unfortunately, these copies do not possess the clarity of the original x-ray negatives, but the originals are available at LLNL for inspection by interested investigators. The first print is a 200-keV image focused on the damaged gas tube from the top of the cell cap through the Swagelok fitting. In the original negative, the tube appeared unobstructed over the length of this segment. The second radiograph is a 4-MeV image showing the Teflon end-piece within the cell cap; the end-piece was definitely skewed within the cap enclosure. The third radiograph is analogous to the second, except oriented at an angle of 135° relative to the former. The interiors of the gas tube and fitting were more apparent with this view.

NDE Job Order Request Form

Job Order No.	Reference No.	Date	Account No.	Location
46048	46048	05/27/92	5388 – 18	B239

Customer
Grant , Pat

Customer Serial No.
NONE

Nuclear Data (Y/N)
N

Document No:

Part Class. (U,C,S): U

Item/Description
SRI-MAIN STAINLESS STEEL CELL AND DETACHED CELL BASE

Quantity
2

No. of Film
0

Information Requested
RADIOGRAPH FOR ALL ANOMALIES.

Hazardous Material - (Y/N) - if Y explain: N

Handling Precautions-(Y/N)- if Y explain: Y -

Marking Restrictions-(Y/N)- if Y explain: Y -

Suggested Inspection Method(s):
RT (and)

Lead Technician: Hester
2nd Technician: Ford
Coordinator (deliver to): Grant

Report Draft

Job Order: 46048
Account No. 5388-18
May 29, 1992

TO: Pat Grant - L-234

FROM: L. O. Hester/W. T. Fritts/K. W. Dolan

SUBJECT: SRI Cell Inspection

Summary

An investigative radiographic inspection was performed on stainless steel vessel parts provided by Stanford Research Institute, Palo Alto, California. The purpose of the inspection was to image the components of the vessel. The inspection was performed in accordance with general radiographic guidelines used as standard practice in the LLNL/NDE Section. However, because of limited inspection time, this inspection should be accepted as a "best effort" basis.

Two parts, the Main Cell Body with attached Gas Tube and the Detached Cell Base, were inspected. Because of varying part thickness and part configuration, several radiographic parameters were used. This provided varying degrees of image detail within the Main Body Cell. The inspection procedures follow.

Gas Tube

Four orientational views, 0, 45, 90, and 135° (part rotated counter clockwise), were made using the following radiographic parameters, 200 kVp energy, 5 mA, 5 ft. TFD (target-to-film distance) and a film packet consisting of .005 Pb/Kodak M/.010 Pb. The exposure time was one minute. The viewable length of the tube showed a small indentation in the 0° orientation. Also noted were 3-5 small dark spots in the film image of the viewable tube length. Dark spots in film images normally indicate loss of material, e.g. nicks, gouges, pitting, scratches, etc. In the viewable length, the tube appears to be free of obstructions. Features of the tube capping device and the tube inside the device are visible in the film images. The tube appears to be expanded, i.e. flared out, inside the capping device.

Main Cell Body

The above orientational views were also used in the inspection of the Main Cell Body. The radiographic parameters included the following: 4 MeV energy, 24 ft. TFD and a film pack of .020 Pb/Kodak SR film. Three sets of radiographs, each with the above orientational views, were exposed to provide radiographic coverage of the Main Cell Body. The exposures were 1.5 kilorad (3.3 min.),

2 kilorad (4.4 min.) and 3 kilorad (6.6 min.). Internal features including wires and the teflon plate were easily imaged. Partial image of the upper steel cap plate and tube entrance was visible.

Detached Cell Base

Two radiographic exposures at one orientational view, were made of this part. The parameters were 200 keV energy, 5 mA, 5 ft. target-to-film-distance, .005 Pb/Kodak M/.010 Pb film pack and exposures of one and two minutes. A small indentation was located at the center with surface pitting at the 6 o'clock position of this part. Both can be seen by radiographic and visual inspection. The rough circular edge of the part was also imaged in the radiograph.

Conclusions

Two stainless steel parts were inspected using standard LLNL/NDE radiographic inspection procedures. The two parts were the Main Cell Body with attached Gas Tube and the Detached Cell Base . Multiple exposures were taken and a number of orientations were used with each part to provide radiographic coverage of part details. The inspections were done on a best effort basis due to limited time. In the viewable length of the tube, no apparent obstructions were observed in the film images. A few (3-5) small dark spots were noted in the viewable length of the tube, which are normally indications of loss of material, e.g. nicks, pits, scratches, etc. Features of the tube capping device and the tube inside the device are visible in the film images. The tube appears to be expanded, i.e. flared out, inside the capping device.

As noted in our conversations, additional information may be obtained on the tube entry feature in the Main Body Cell with collimated views. This was not done due to lack of time. Additional radiographs following cell disassembly should also be considered to provide added information.

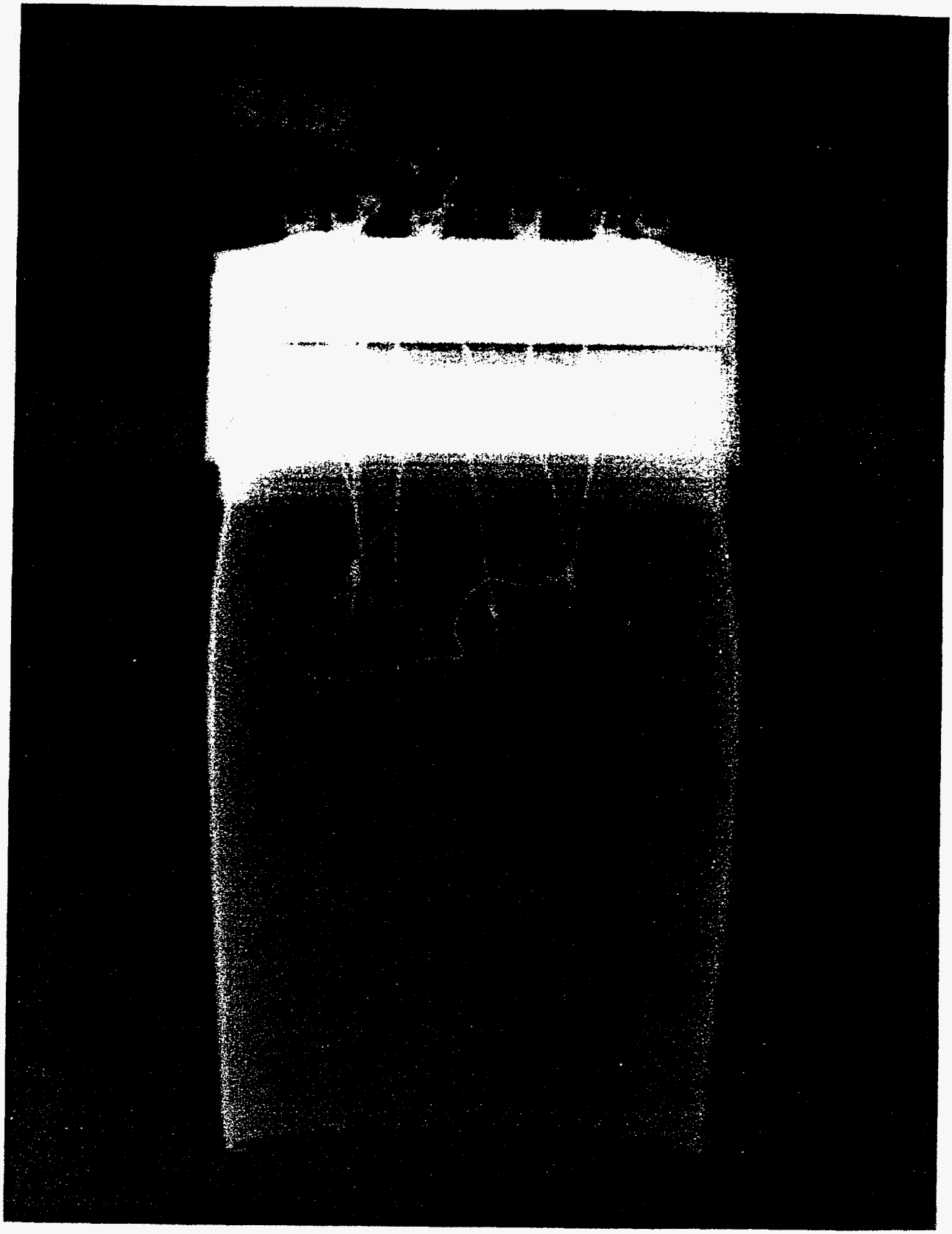

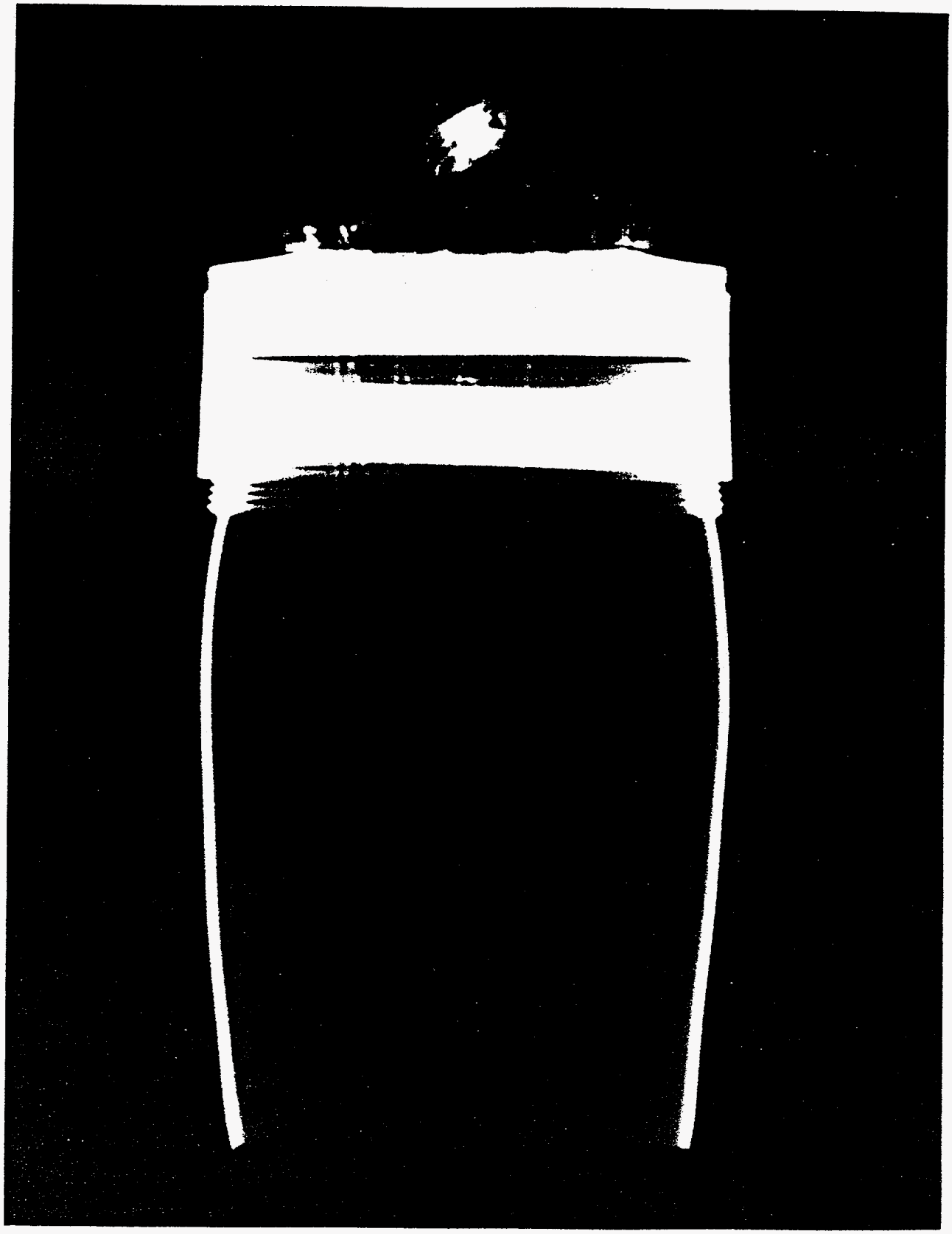

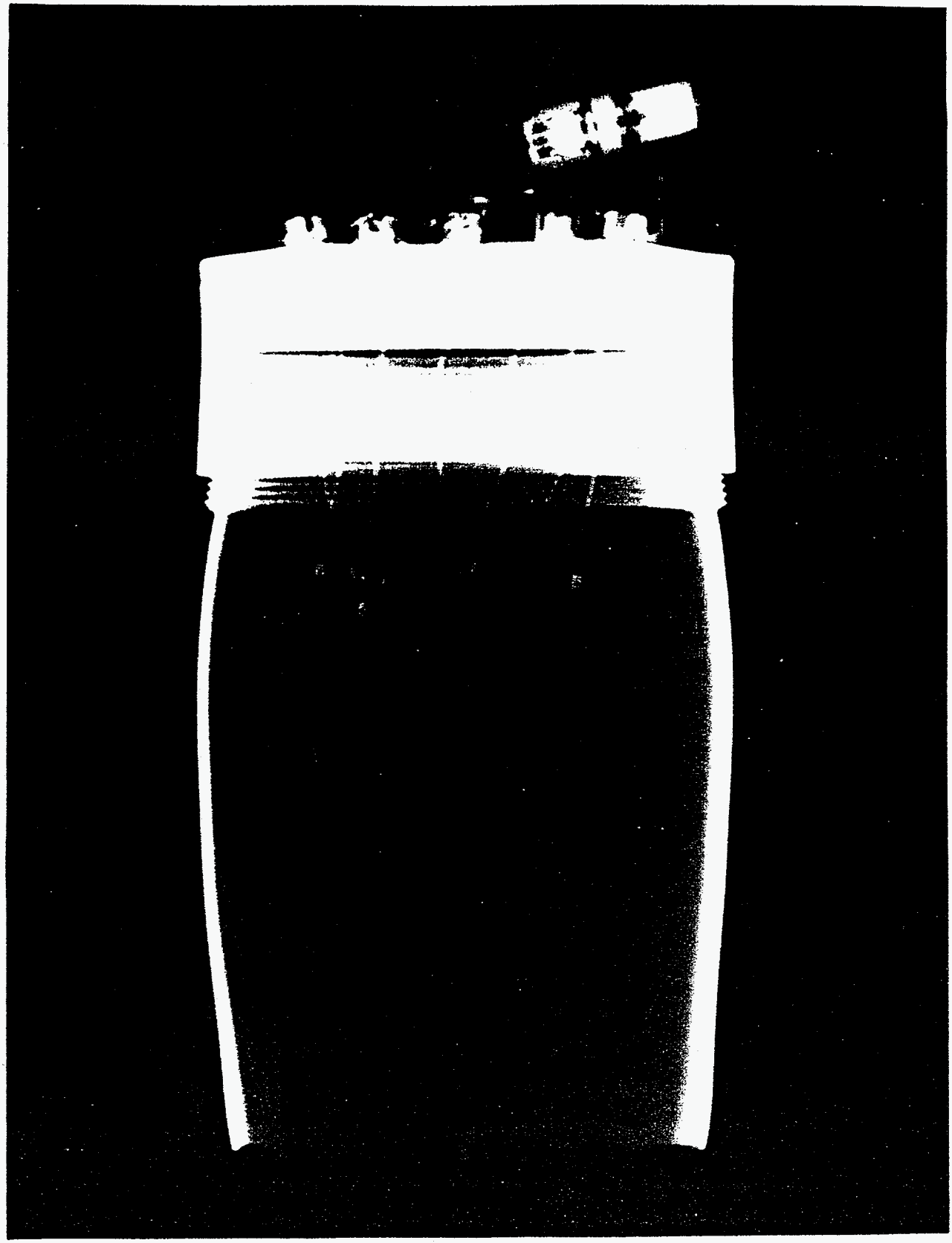

Post-Explosion Cell Dimensions

Accurate measurements of the dimensions of the stainless steel cell vessel and the detached cell base were made. These measurements included the thickness of the cell wall at strategic locations, and the results of this work are summarized on the LLNL sketch sheets attached to this section of the report.

Metallurgical Analyses

The steel cell vessel and detached base were sectioned for metallurgical analyses via scanning electron microscopy (SEM) and metallography. Both the base metal and the weld material were found to be free of significant impurities or contamination. The weld at maximum penetration missed the center-line of the step joint by 0.5-1.3 mm, as measured at three different debris locations, and the weld penetration was incomplete. Four separate measurements of weld penetrations gave an average value of 54%.

No evidence of corrosion or hydrogen embrittlement was observed. Interrogation of the debris by SEM revealed dimple-rupture and wavy-glide features, thus indicating mechanisms of ductile failure from overload of the weld-parent metal intersection at the cell base. The region of initiation of the vessel failure was identified.

A copy of the complete metallurgical report is presented as an addendum to this section of the report. Also included are appropriate photomicrographs at magnifications from 32-100×, and SEM micrographs at magnifications of approximately 500 and 1000×.

SUBJECT	SKETCH	JOB ORDER INFORMATION		
SRI VESSEL BODY & CAP	LAWRENCE LIVERMORE LABORATORY UNIVERSITY OF CALIFORNIA	JOB NO.		TAG NO.
DRAWN BY C. BIANCHINI		SERIAL NO.		NO. REQD.
DATE 6-2-92 / BUILDING NO. / ROOM NO.	APPROVED BY / DATE	DATE ISSUED		DATE REQD.
		DELIVER TO		

TOLERANCES ±.005

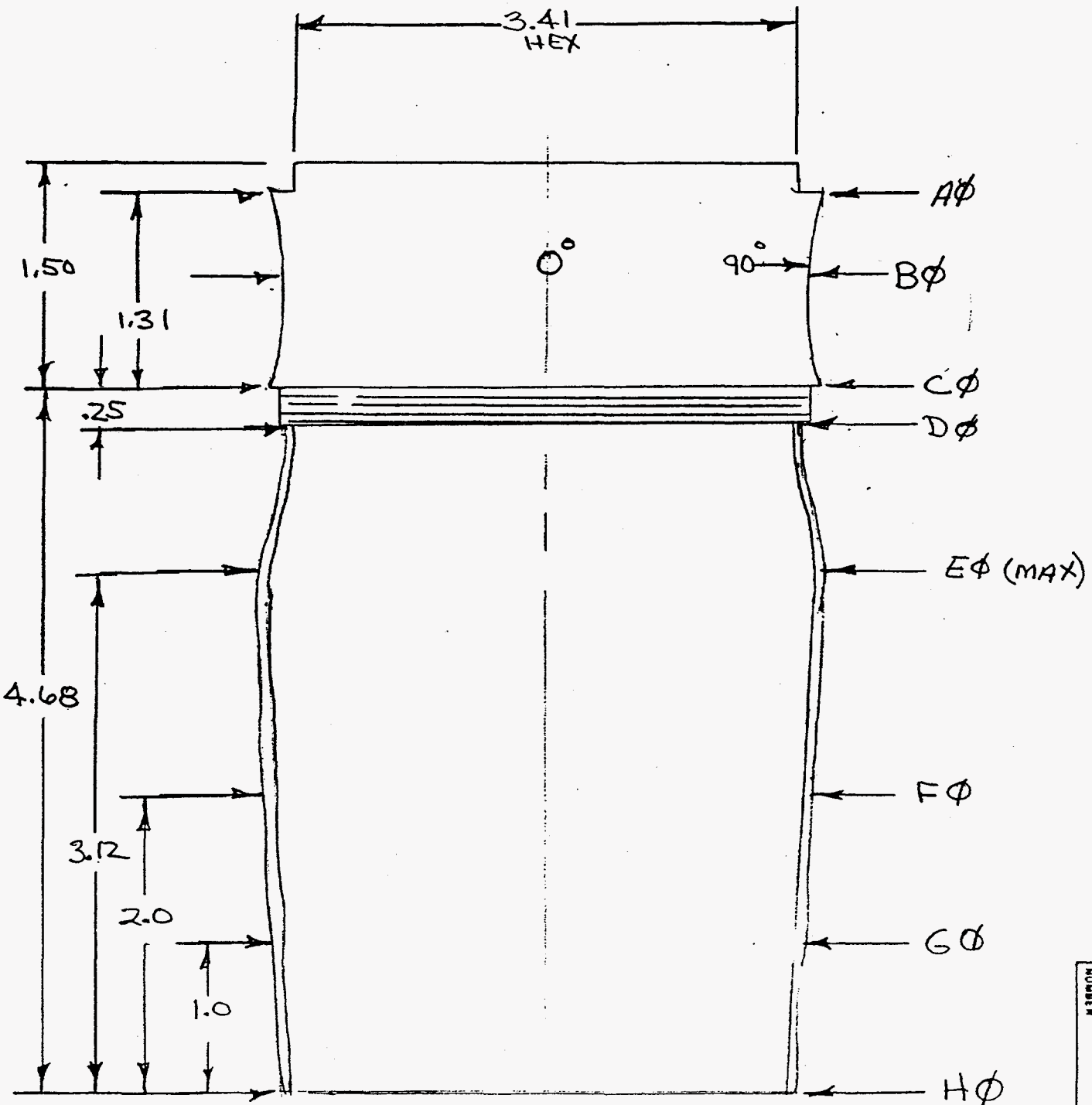

NOT TO SCALE

SKETCH NUMBER

112 (REV.8/71)

SKETCH NUMBER

TOLERANCES ±.005			TOLERANCES ±.0005			
POSITION Ø	DEGREES 0 – 180 Ø	DEGREES 90 – 270 Ø	WALL THICKNESS @ 0°	WALL THICKNESS @ 90°	WALL THICKNESS @ 180°	WALL THICKNESS @ 270°
A	3.690	3.685	—	—	—	—
B	3.695	3.700	—	—	—	—
C	3.735	3.750	—	—	—	—
D	3.487	3.504	—	—	—	—
E	3.710	3.710	.0625	.0657	.0657	.0641
F	3.620	3.600	.0638	.0675	.0673	.0677
G	3.457	3.427	.0669	.0703	.0695	.0717
H	3.298	* 3.207	.0634	.0751	0780	.0751

* BADLY OUT OF ROUND (EGG SHAPED FROM IMPACT)

SUBJECT: SRI VESSEL
DRAWN BY: G. BIANCHINI
DATE: 6-2-92
BUILDING NO.
ROOM NO.
SKETCH
LAWRENCE LIVERMORE LABORATORY
UNIVERSITY OF CALIFORNIA
APPROVED BY
DATE
JOB ORDER INFORMATION
JOB NO.
SERIAL NO.
DATE ISSUED
DELIVER TO
T&A NO.
NO. REQD.
DATE REQD.

L-112 (REV.8/71)

SUBJECT: SRI VESSEL (BOTTOM)

DRAWN BY: G. BIANCHINI

DATE: 6-2-92

BUILDING NO.:

ROOM NO.:

SKETCH

LAWRENCE LIVERMORE LABORATORY
UNIVERSITY OF CALIFORNIA

APPROVED BY:

DATE:

JOB ORDER INFORMATION

JOB NO.:

TAG NO.:

SERIAL NO.:

NO. REQD.:

DATE ISSUED:

DATE REQD.:

DELIVER TO:

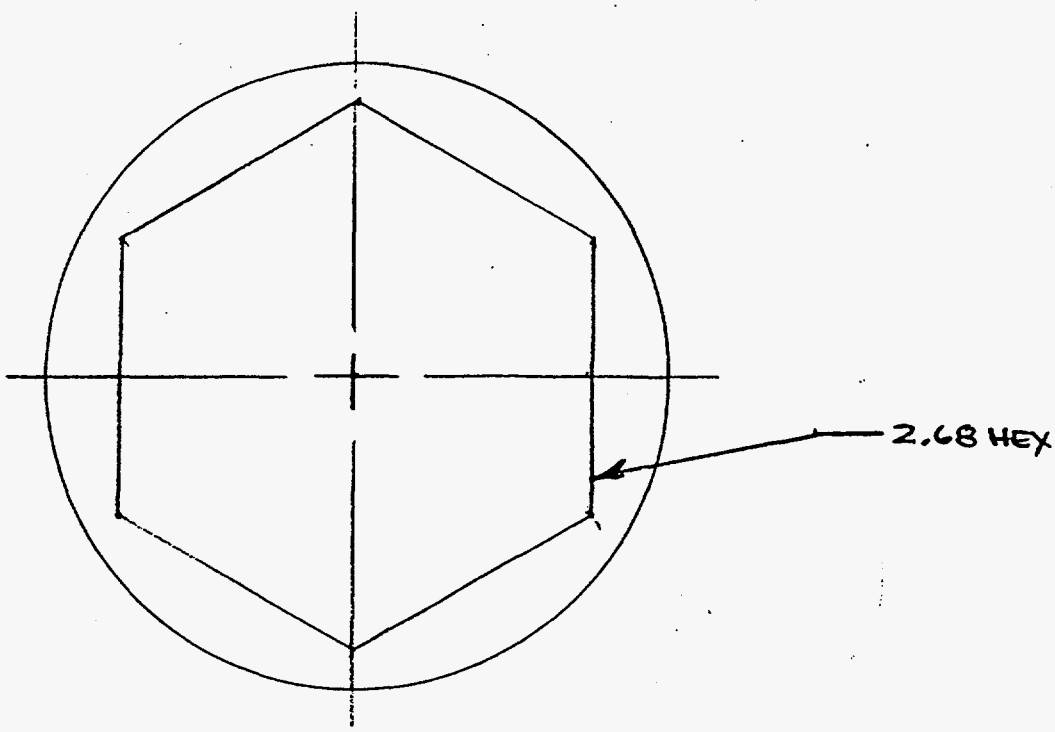

AVERAGE DISPLACEMENT FROM CENTER TO EDGE OF HEX FLAT

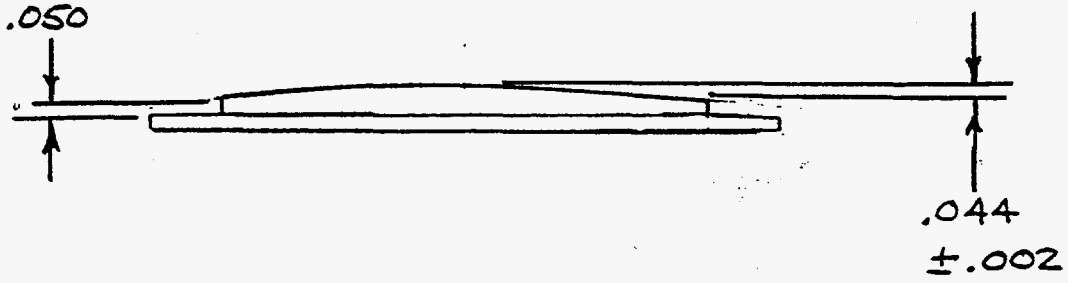

NOT TO SCALE

THICKNESS OF BOTTOM				
POSITION FROM CENTER	0°	90°	180°	270°
0	.119	—	—	—
1/2"	.1175	.1175	.1172	.1173
1"	—	—	.1168	—

MISSING measurements @ 1" are a result of metalography specimen HAD BEEN REMOVED IN THAT AREA

SKETCH NUMBER

L-112 (REV.8/71)

SUBJECT SRI VESSEL ASSY

DRAWN BY G. BIANCHINI

DATE 6-2-92 | BUILDING NO. | ROOM NO.

SKETCH

LAWRENCE LIVERMORE LABORATORY
UNIVERSITY OF CALIFORNIA

APPROVED BY | DATE

JOB ORDER INFORMATION

JOB NO. | TAG NO.
SERIAL NO. | NO. REQD.
DATE ISSUED | DATE REQD.
DELIVER TO

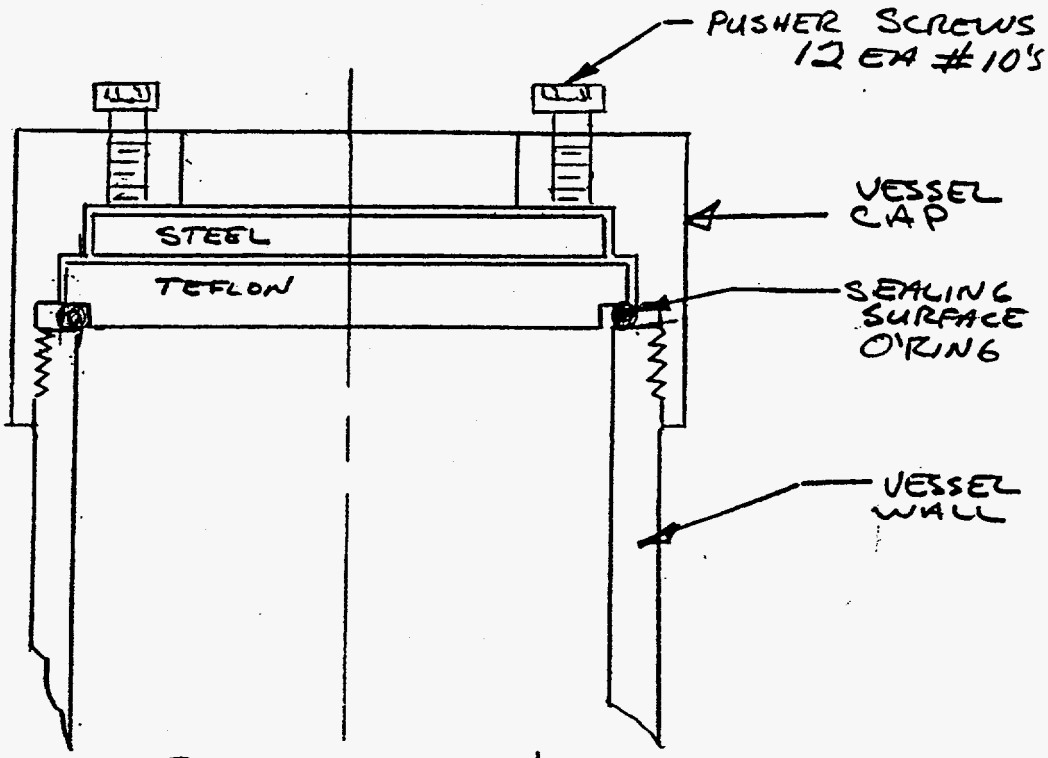

BOTTOM WELDED IN

NOT TO SCALE

THIS SKETCH IS ONLY AN ASSUMPTION OF THE END CAP ASSEMBLY AFTER VIEWING THE PROVIDED RADIOGRAPHS. PRIOR TO DISASSEMBLY

SKETCH NUMBER

L-112 (REV.8/71)

Interdepartmental letterhead

Mail Station L - 342

Ext: 2-7064

June 4, 1992
MTE 92-041

TO : Patrick Grant

FROM: Richard Vandervoort, Robert Kershaw, Edwin Sedillo

SUBJECT: **Metallurgical Analysis of Stanford Research Institute Experimental Vessel**

A metallurgical examination was made on the cylinder and base plate that was part of the system in a Stanford Research Institute (SRI) experiment. The failure surface of the base plate was examined in an International Scientific Instruments (ISI-DS 130) Scanning Electron Microscope (SEM). Sections were then cut from the cylinder and base plate. They were taken at the arbitrary reference point on the cylinder labeled 0° and then at 90° and finally at 180° moving in a counter clockwise direction, looking from the bottom of the base plate to the top of the cylinder. It was necessary to re-orient the base plate with respect to the cylinder. The failure surface at the 90° mark on the external surface of the base plate corresponded to the failure surface at the 0° mark on the cylinder. This 90° rotation gave an exact match of failure surface contours on the cylinder and base plate. The sections were mounted in bakelite, mechanically polished, and then electro-etched in a saturated solution of oxalic acid at 10V for one minute. The sections were mounted so that material from the welded joint to the interior base metal could be viewed (Fig. 1).

The polished and etched samples were examined in a Reichert-Jung metallograph at magnifications from 30 to 200x. The base metal, identified as 316 stainless steel (see section on materials characterization and structural analysis) was of good quality and free from significant impurity inclusions or carbide precipitates. The multi-pass weld was also free from contamination. We estimate that 8 passes were made to complete the seal. We found that the weld bead at maximum penetration had missed the center line of the step joint by 0.5, 1.3, and 0.5mm at the 0°, 90°, and 180° positions respectively. In addition, there was incomplete weld penetration. Four measurements gave weld penetrations of 55%, 43%, 54%, and 63% with an average value of 54% (Figs. 2-4). The crack propagated thru the base metal near the parent metal-weld interface. Ferrite

University of California
Lawrence Livermore
National Laboratory

measurements showed ferrite contents of 0.25% to 0.75% in the vicinity of the weld. No ferrite was detected elsewhere in the parent metal. There was no evidence of corrosion, stress corrosion cracking, or hydrogen embrittlement. The delta ferrite in the area at the root of the weld (Fig. 5) played no role in the failure. We concluded that the failure resulted from an overload in the weld-parent metal region of the base plate-cylinder joint.

The total failure surface of the base plate was examined in the SEM. The failure mode was consistent around the circumference of the base plate. The fracture was mixed mode and showed both dimple rupture and wavy glide failure (Figs. 6-11). These scanning electron micrographs correspond to the 0°, 90°, and 180° areas studied with metallography (Figs. 2-4). The dimple rupture and wavy glide are both ductile failure mechanisms. This observation is in accord with the metallography results and further substantiates that the failure resulted from an overload of the vessel at the weld-parent metal interface. The stress at the interface was the highest anywhere in the vessel due to the incomplete weld penetration and the stress concentrations at the unfused step joint. The origin of the failure appeared to be in the 0° area. The weld was thinnest in this area. Note that the failure surface is heavily ridged here (Fig. 12) as compared with the other SEM micrographs (Figs. 6-11). This was the only area that had this type of shearing, indicating a complex state of stress before crack initiation.

Attachments

Distribution:

G. Gallegos, L-352
R. Jandrisevits, L-144
J. Kass, L-350
S. Root, L-144

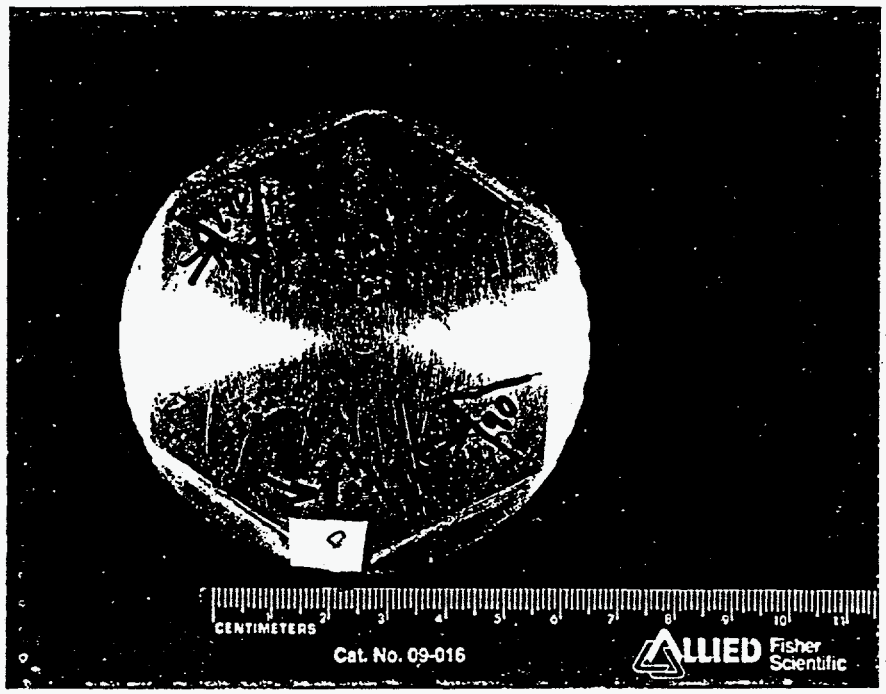

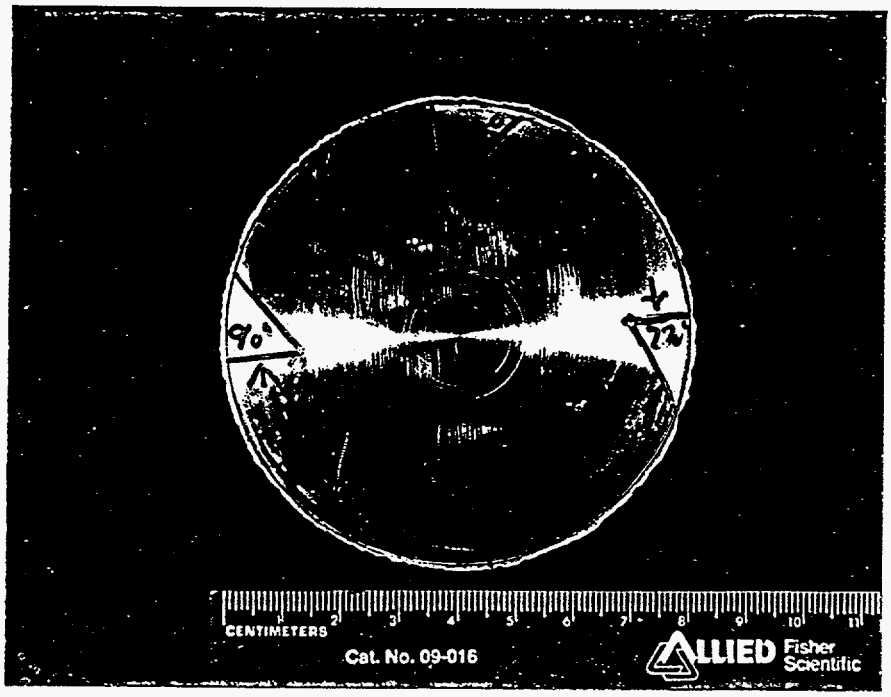

FIGURE 1

BASE OF VESSEL

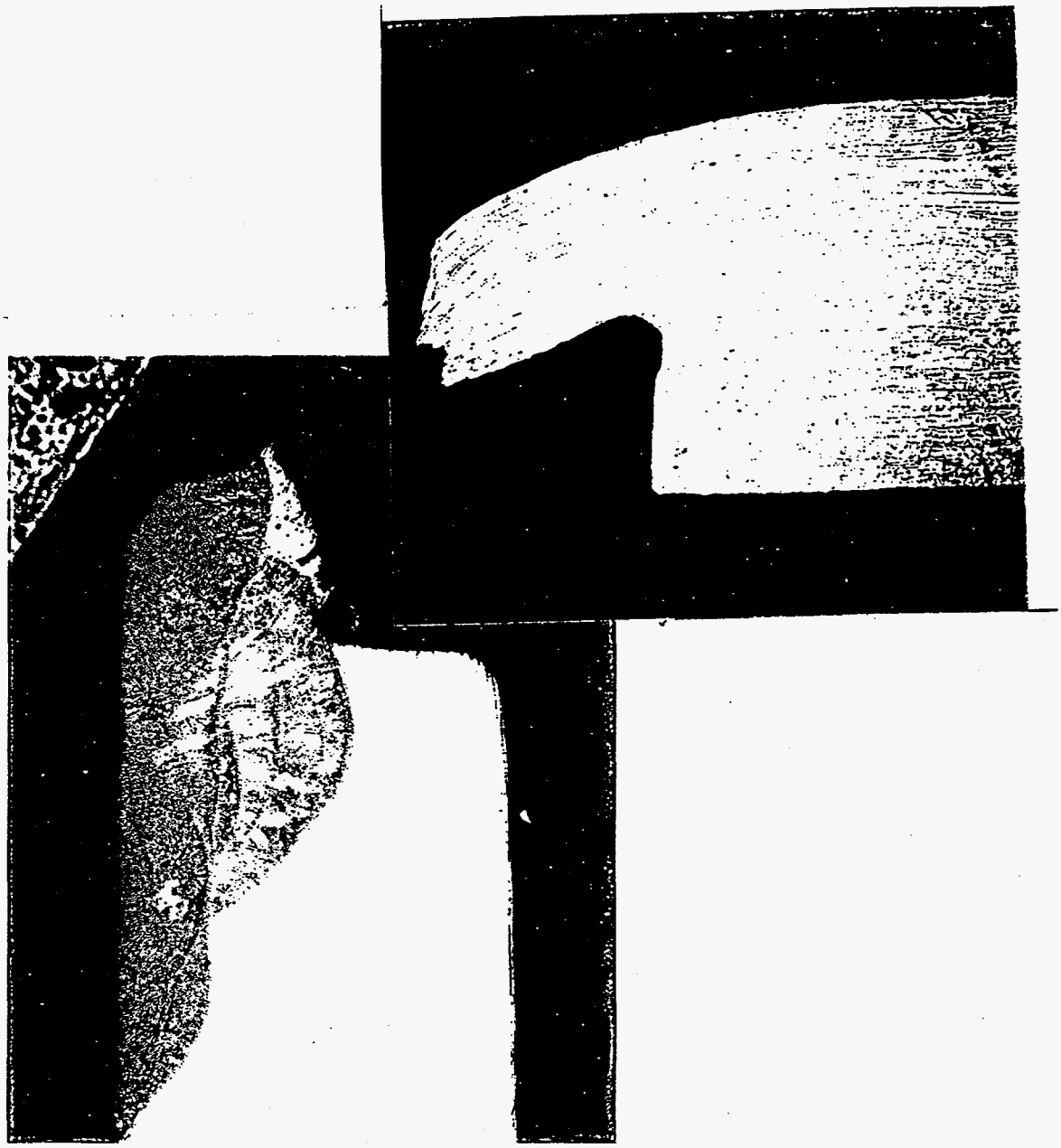

FIGURE 2

0 DEGREES 32X

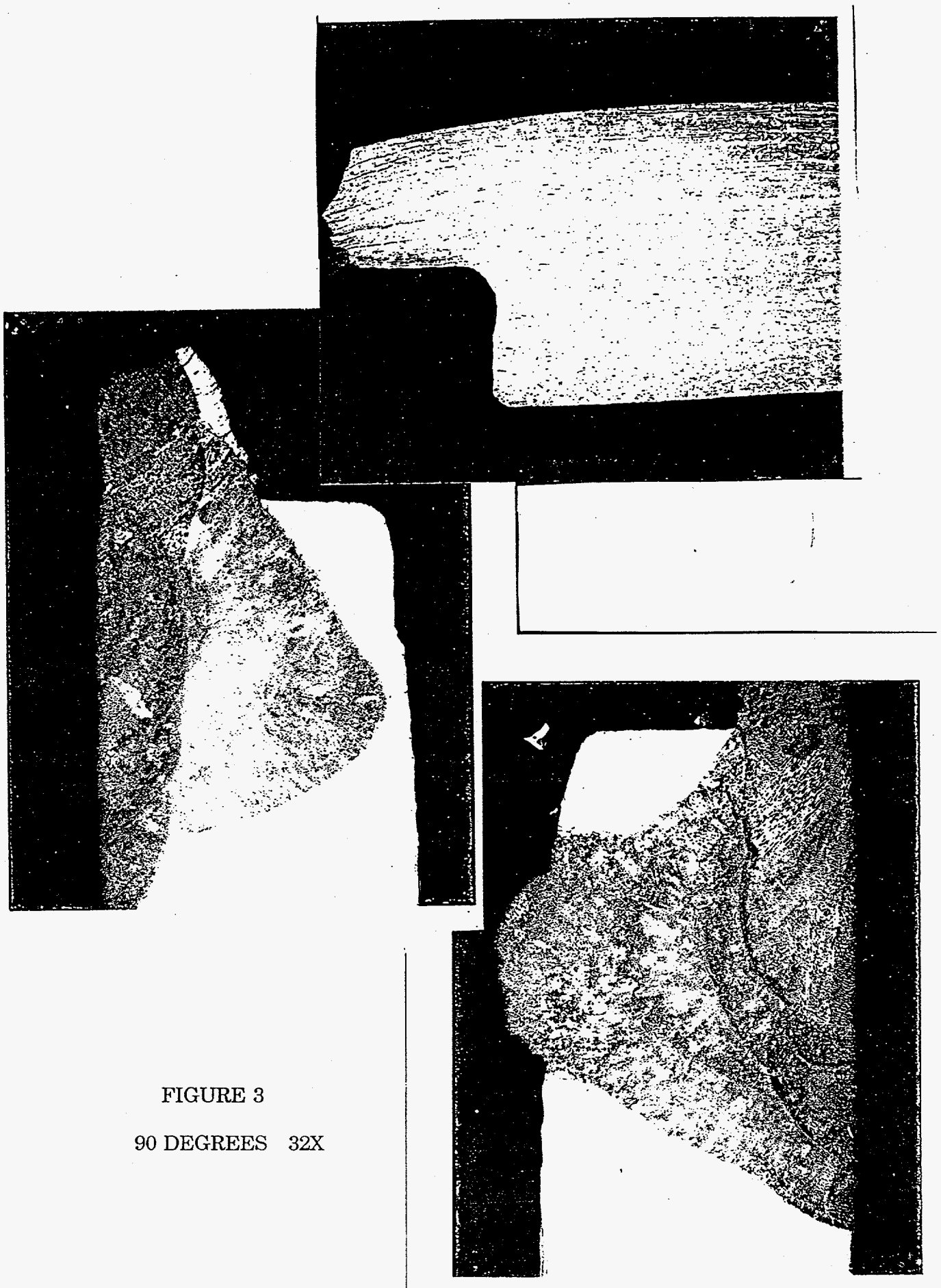

FIGURE 3

90 DEGREES 32X

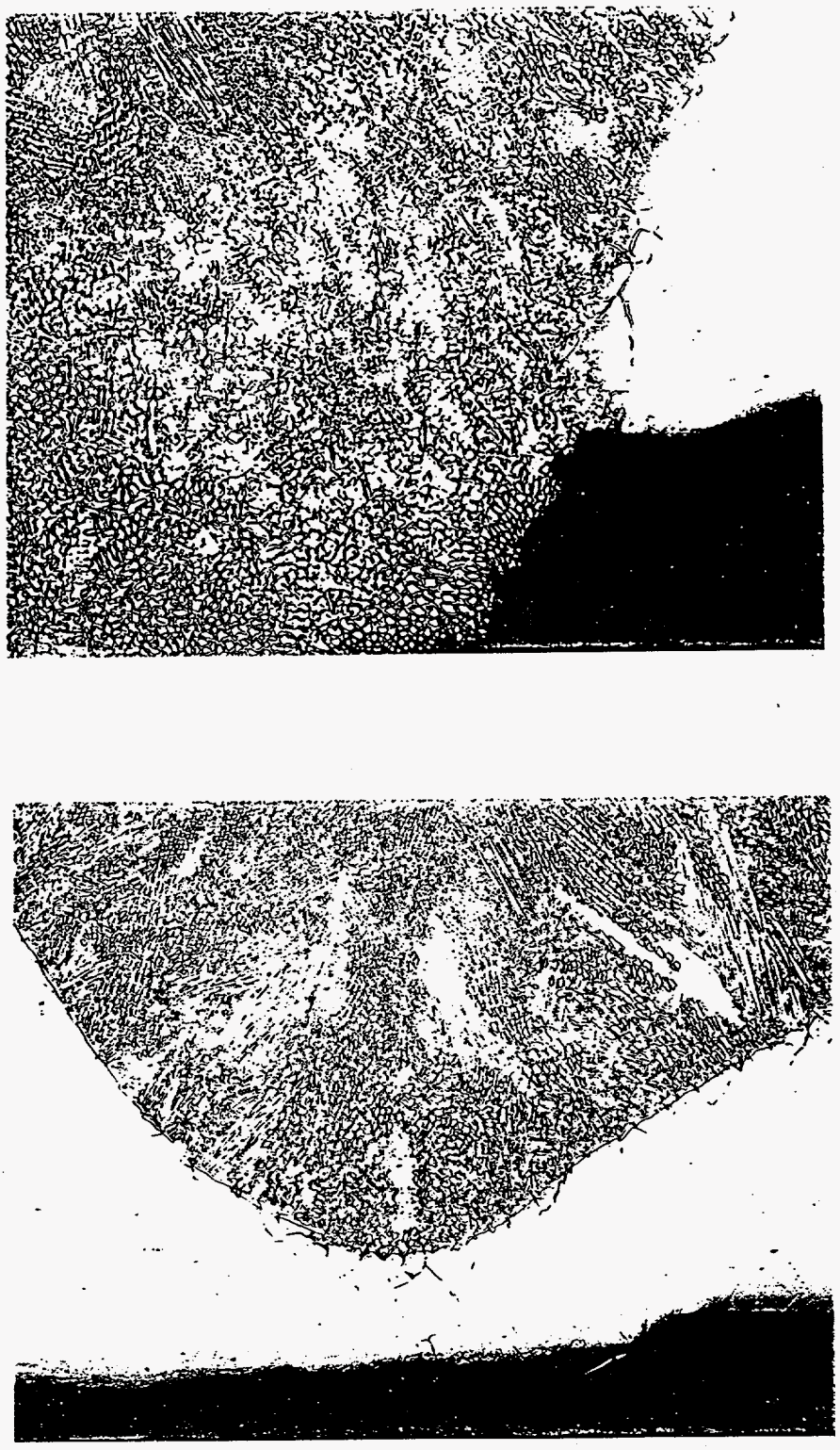

FIGURE 5

90 DEGREES 100X

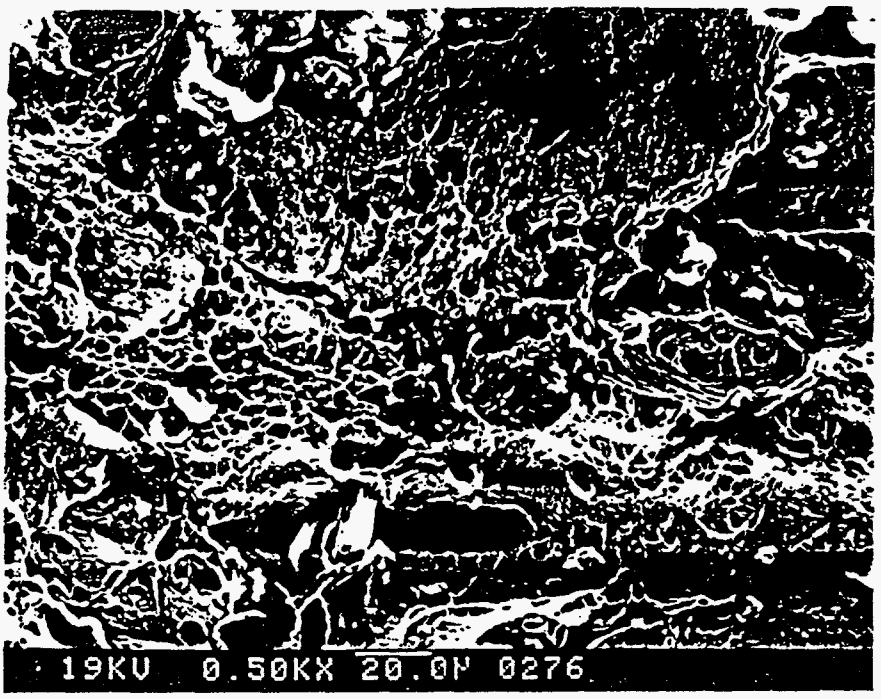

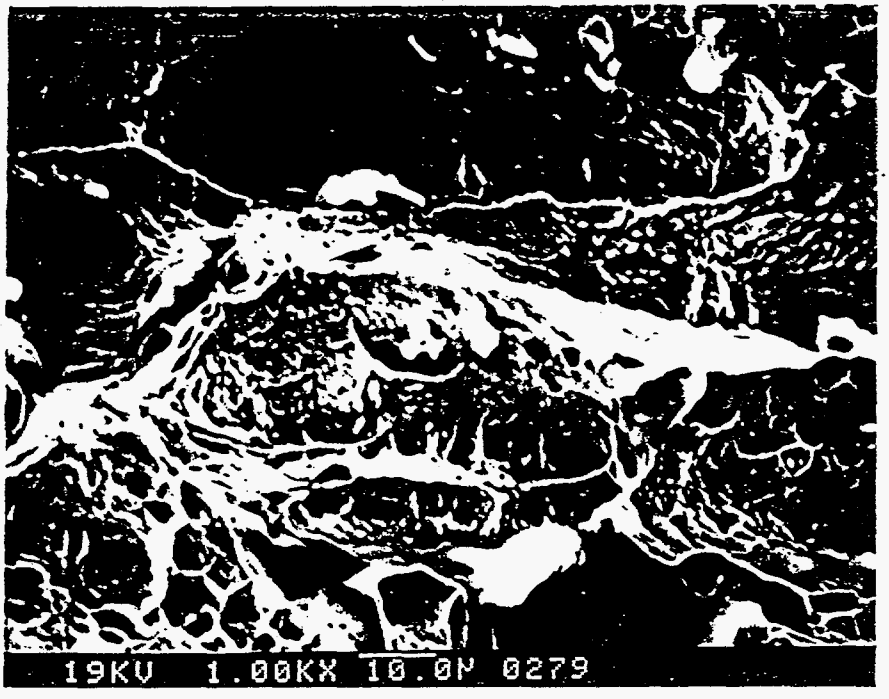

FIGURE 6

0 DEGREES

INNER WALL

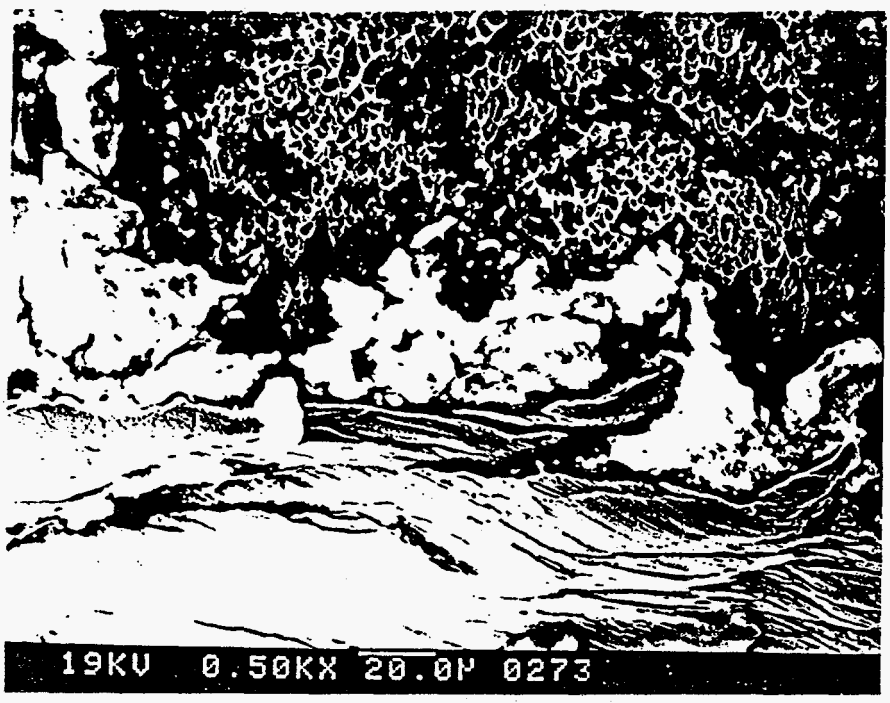

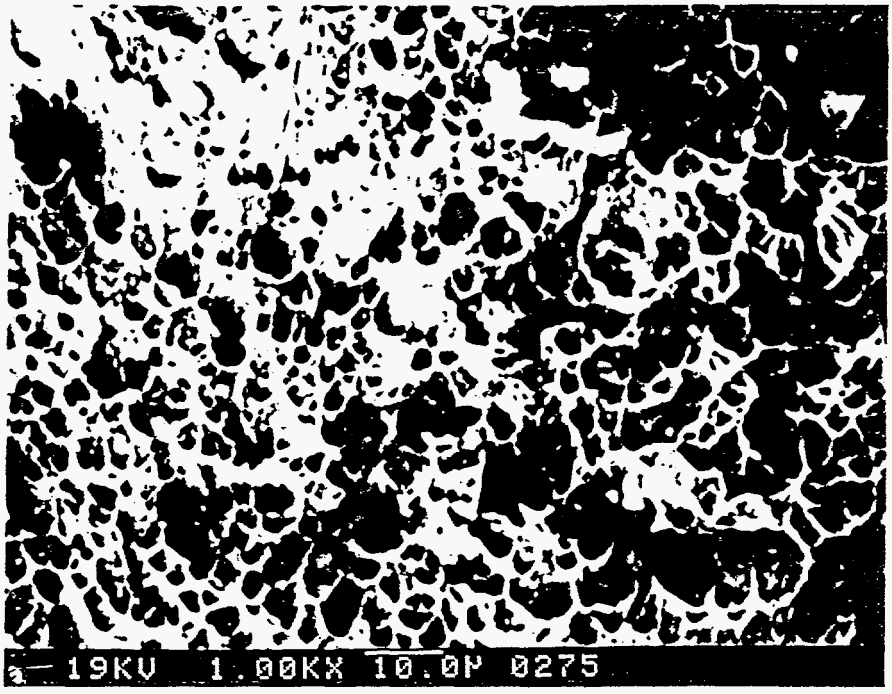

FIGURE 7

0 DEGREES

OUTER WALL

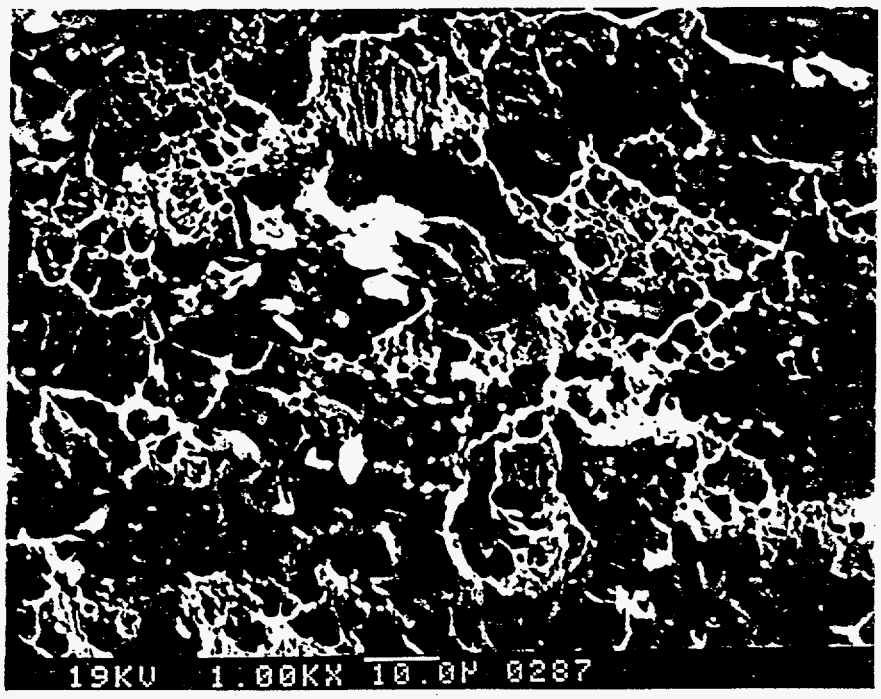

FIGURE 8

90 DEGREES

INNER WALL

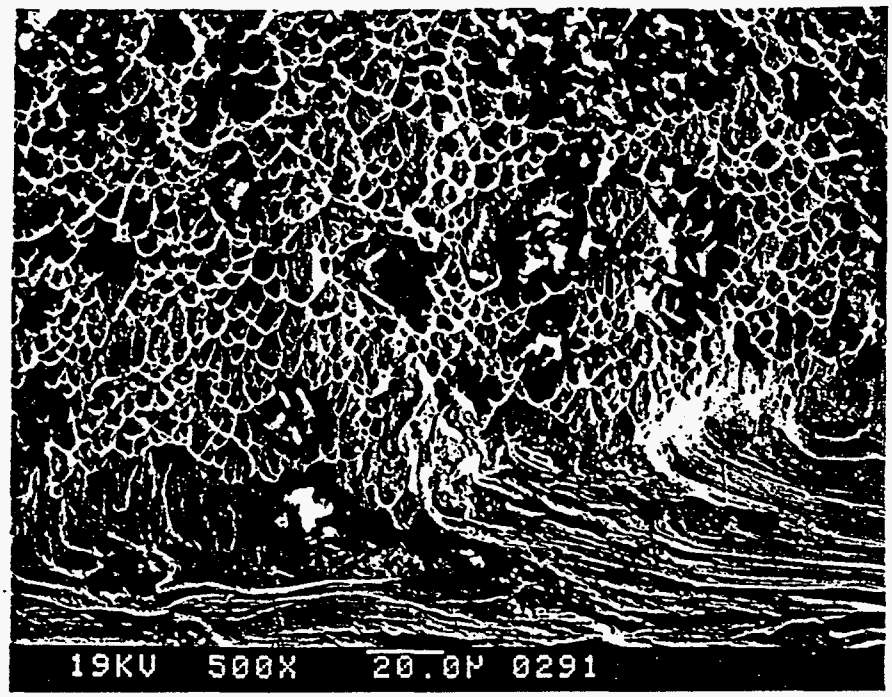

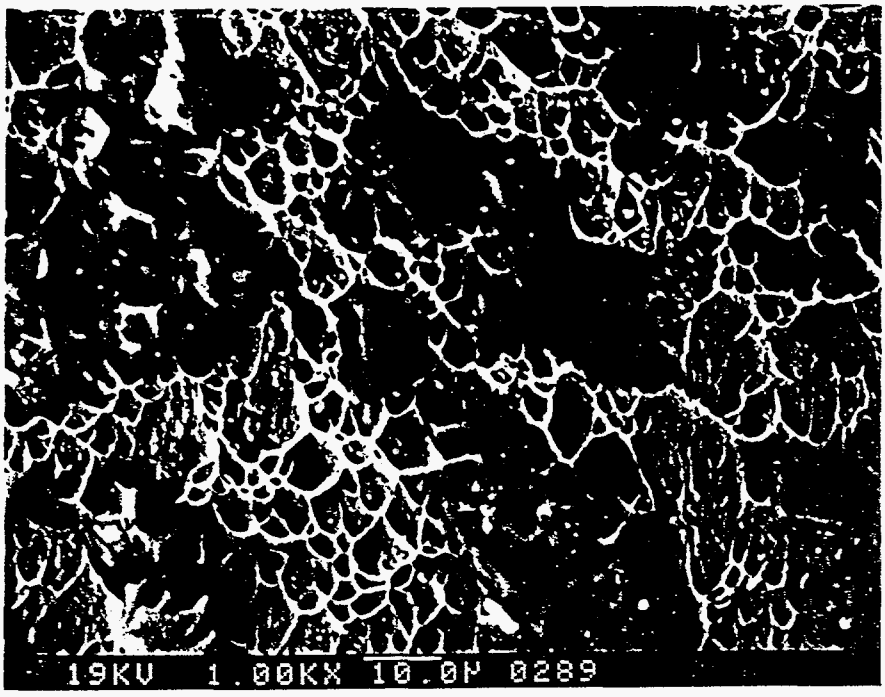

FIGURE 9

90 DEGREES

OUTER WALL

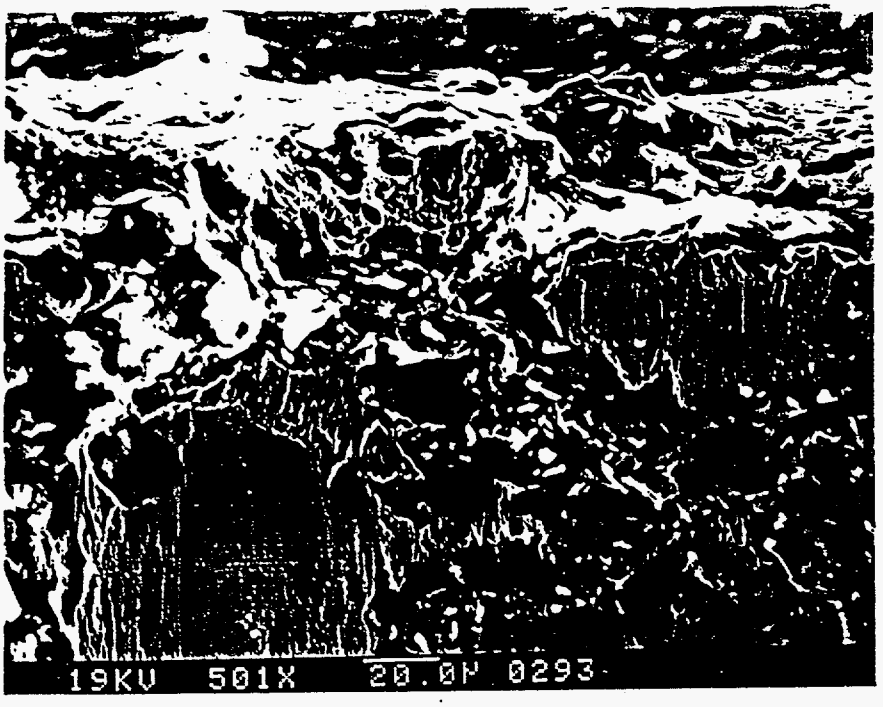

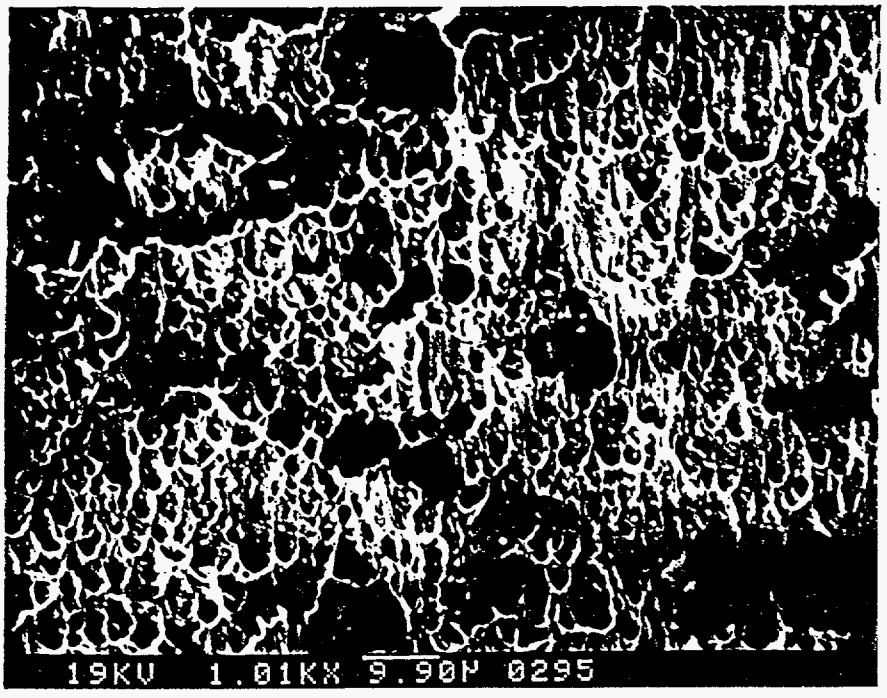

FIGURE 10

180 DEGREES

INNER WALL

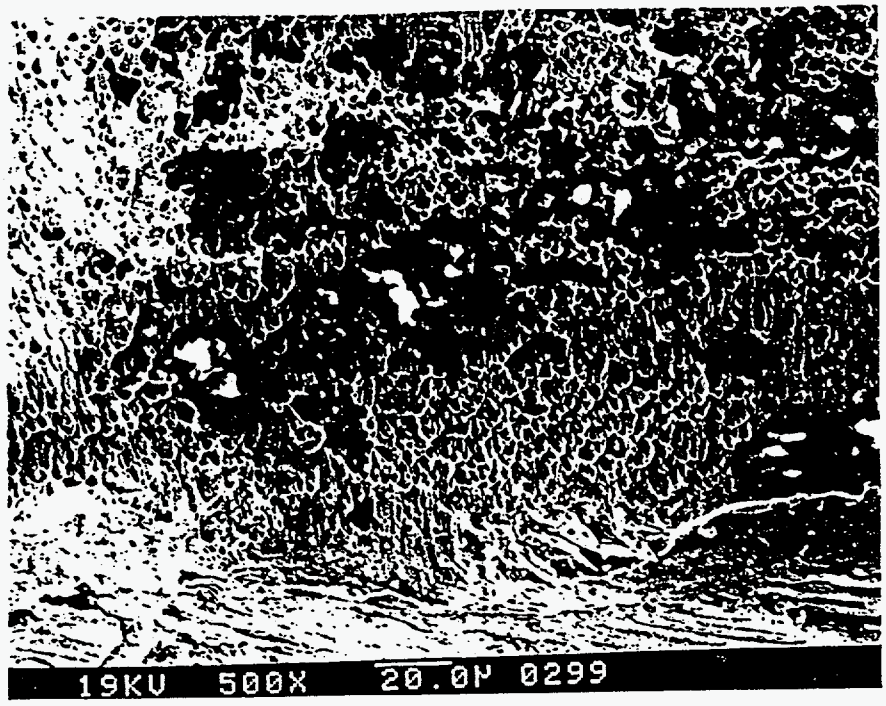

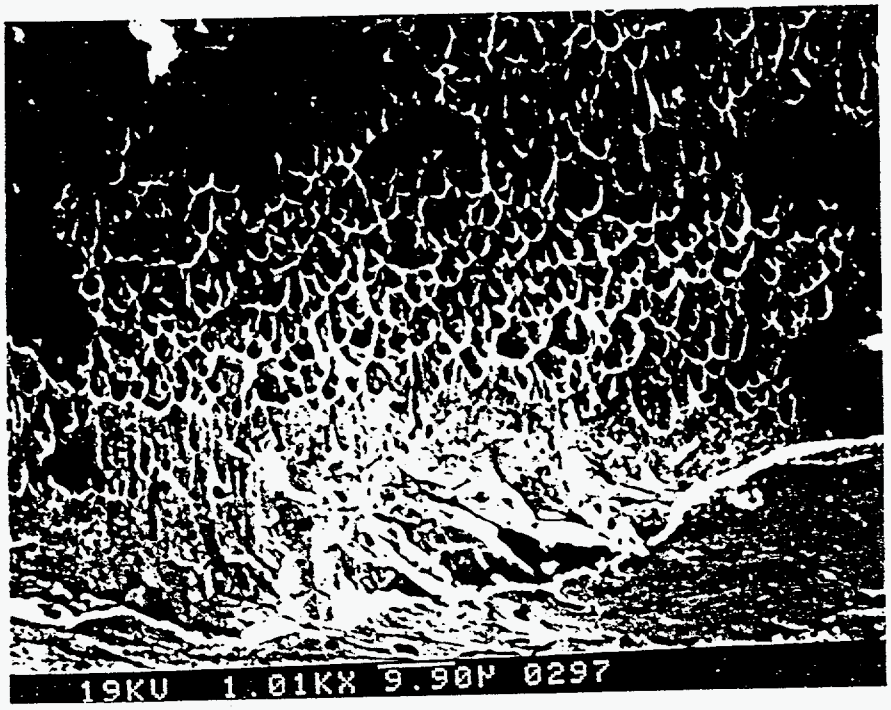

FIGURE 11

180 DEGREES

OUTER WALL

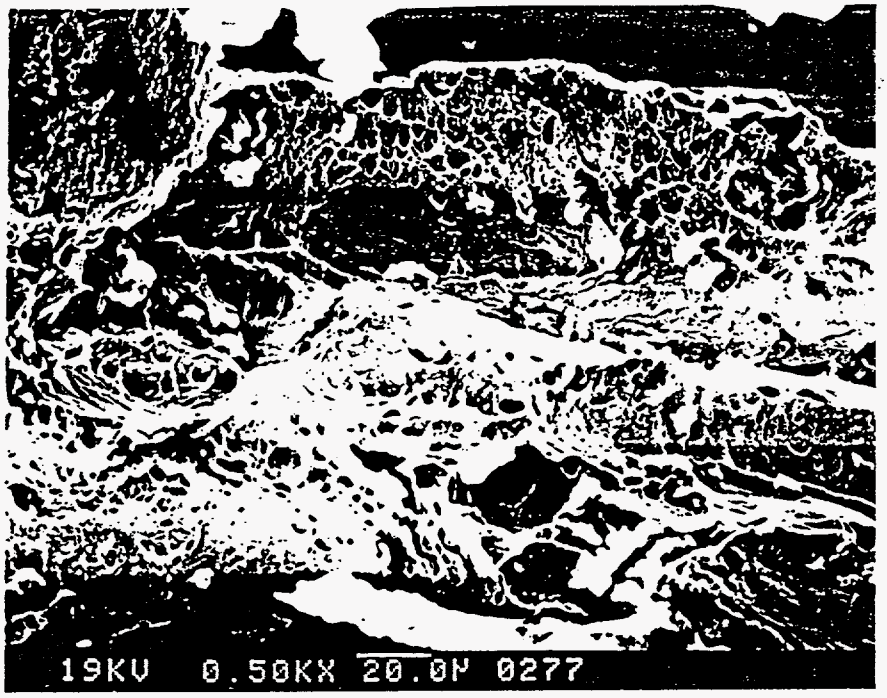

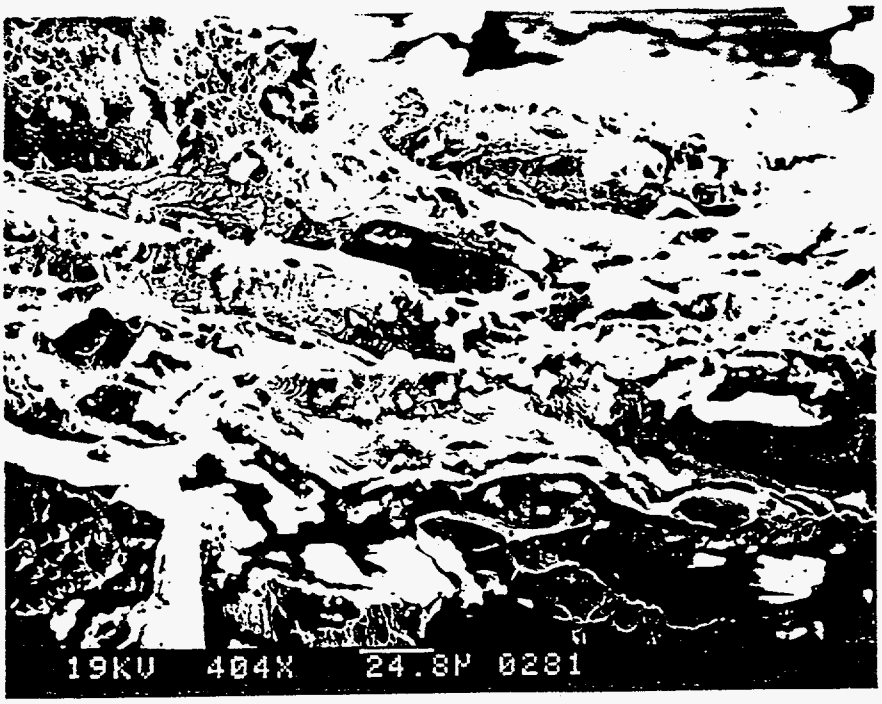

FIGURE 12

0 DEGREES

INNER WALL

SUMMARY

SUMMARY

Selected components of explosion debris from the SRI incident of January 2, 1992 were subjected to forensic analyses at LLNL to elucidate potential causes of, or contributing factors to, the explosion. Interrogation of the debris by LLNL encompassed nuclear, chemical, physical, and materials investigations.

Nuclear studies for the determination of tritium and neutron-activation products in stainless steel and brass were negative, down to detection limits of the order of pCi of radioactivity. No evidence of signature species indicative of orthodox nuclear events was detected.

The inorganic and particulate analyses were likewise negative with respect to residues of unexpected chemical species. Such target compounds included conventional explosives, accelerants, propellants, or any exceptional industrial chemicals. In the absence of prior knowledge of the details of this incident, the sensitive detection at LLNL of trace amounts of Pt, Pd, Li, and enriched D/H in the debris would have led to the identification of the apparatus as a "cold fusion" experiment with a high degree of probability and confidence.

The GC-MS analyses of trace organic components in the explosion debris provided perhaps the most interesting results obtained at LLNL. Although no evidence of organic explosives, oxidizers, or other unusual compounds was detected, the presence of a hydrocarbon oil in the interior of the electrochemical cell was established. While it is possible that this oil originated through post-explosion contamination of the debris, it is likely that its source was lubricating fluid from the machining of the metal cell components. If residues of organic oils are present during electrolysis experiments, the potential exists for an explosive reaction in the increasingly enriched oxygen atmosphere within the headspace of a metal cell.

Materials characterization identified the type of stainless steel used in the manufacture of the electrolytic cell as one relatively high in Mo concentration, probably type 316. Exact measurements of various cell dimensions following the explosion were made and presented in the body of the report. Metallurgical analyses of the cell vessel wall and the detached base provided no evidence of corrosion or hydrogen embrittlement, leaving only ductile failure of the weld as contributing to the incident. The weld was found to have missed the center-line of the step joint, and the average penetration of the weld was measured to be 54%.